



**HAL**  
open science

## Storm surge and tsunami deposits along the Moroccan coasts: state of the art and future perspectives

Otmane Khalfaoui, Laurent Dezileau, Samira Mellas, Nadia Mhammdi, Fida Medina, Meryem Mojtahid, Otmane Raji, Hajar El Talibi, Jean-Philippe Degeai, Khalid El Khalidi, et al.

### ► To cite this version:

Otmane Khalfaoui, Laurent Dezileau, Samira Mellas, Nadia Mhammdi, Fida Medina, et al.. Storm surge and tsunami deposits along the Moroccan coasts: state of the art and future perspectives. *Natural Hazards*, 2023, 10.1007/s11069-023-05940-z . hal-04077804

**HAL Id: hal-04077804**

**<https://hal.science/hal-04077804v1>**

Submitted on 3 Jun 2024

**HAL** is a multi-disciplinary open access archive for the deposit and dissemination of scientific research documents, whether they are published or not. The documents may come from teaching and research institutions in France or abroad, or from public or private research centers.

L'archive ouverte pluridisciplinaire **HAL**, est destinée au dépôt et à la diffusion de documents scientifiques de niveau recherche, publiés ou non, émanant des établissements d'enseignement et de recherche français ou étrangers, des laboratoires publics ou privés.



Distributed under a Creative Commons Attribution 4.0 International License

# 1 Storm surge and tsunami deposits along the Moroccan coasts: state of 2 the art and future perspectives

3 Otmane Khalifaoui<sup>1,9\*</sup>, Laurent Dezileau<sup>1</sup>, Nadia Mhammdi<sup>2</sup>, Fida Medina<sup>3</sup>, Meryem Mojtahid<sup>4</sup>, Otmane  
4 Raji<sup>5</sup>, Hajar El Talibi<sup>6</sup>, Samira Mellas<sup>7</sup>, Jean-Philippe Degeai<sup>8</sup>, Khalid El Khalidi<sup>9</sup>, Maria Snoussi<sup>2</sup>,  
5 Zourarah Bendahhou<sup>9</sup>, Khadija Aboumaria<sup>10</sup>

6 <sup>1</sup>Normandie Univ, UNICAEN, UNIROUEN, CNRS, M2C, 14000 Caen, France

7 <sup>2</sup>University Mohammed V in Rabat, Institut Scientifique, Laboratory LGRN and GEOPAC Research Centre, Av. Ibn  
8 Batouta, B.P. 703 Agdal, Rabat, Morocco

9 <sup>3</sup>Moroccan Association of Geosciences, Commission of Natural Hazards, Rabat, Morocco

10 <sup>4</sup>Univ Angers, Univ Nantes, Univ Le Mans, CNRS, LPG, Laboratoire de Planétologie et Géosciences, UMR 6112, 2  
11 Bd Lavoisier, 49045 Angers Cedex, France

12 <sup>5</sup>Geology and Sustainable Mining, Mohammed VI Polytechnic University, Benguerir 43150, Morocco

13 <sup>6</sup>Faculty of Sciences and Techniques of Al Hoceima, Abdelmalek Essaadi University, Al Hoceima, Morocco

14 <sup>7</sup>Institut Supérieur des Etudes Maritimes (ISEM), Casablanca, Morocco

15 <sup>8</sup>ASM UMR 5140, Université Montpellier 3, CNRS, MCC, 34199 Montpellier, France

16 <sup>9</sup>LGMSS URAC-45, University Chouaib Doukkali, El Jadida, Morocco

17 <sup>10</sup>Department of Earth Sciences, Faculty of Sciences and Techniques of Tangier (FST), Abdelmalek Essaadi  
18 University (UAE), Morocco

19

20 **\*Corresponding author: Otmane KHALFAOUI (m.otmanekhalifaoui@gmail.com)**

## 21 Abstract

22 The Moroccan coast is occasionally confronted with marine submersion events caused by storm  
23 surges and tsunamis. The Moroccan historical archives recorded some of these events, such as  
24 the storm surge of 2014 CE and the tsunami of 1755 CE. The latter remains the most destructive  
25 event the country has ever faced, with major human and economic losses recorded mainly  
26 between the two cities of Tangier and Safi. The privileged way to prevent any hazard related to  
27 these events is to study their past occurrences and consequences. However, historical records  
28 are often very scarce to determine their return periods and evaluate their intensities.  
29 Accordingly, the scientific community increasingly uses sedimentary archives from coastal  
30 environments, since they offer a viable alternative to historical archives. Several studies using  
31 this approach have been conducted on the Moroccan coast in recent years; however, until now,  
32 there has been no review dealing with these studies, which is the main objective of this paper.  
33 The present review shows that most of the Moroccan sites containing marine submersion  
34 deposits are located along the Atlantic coast. The Mediterranean coast remain poorly studied  
35 despite the presence of tsunami and storm surge risks. The review draws attention also to the  
36 absence of chronological data for most of the marine submersion deposits recognized up to now

1 along the Moroccan coasts, which is a major issue that prevents the determination of the return  
2 period of these events.

3 Keywords: Tsunami; Storm surge; Boulders; Washover; Morocco; 1755 Lisbon tsunami

## 4 **1. Introduction**

5 About 45% of the world's population lives within 150 km of the coast (Finkl and Makowski  
6 2019). These high human population densities are responsible for the degradation of coastal  
7 zone worldwide, through the overexploitation of natural resources, the urban growth in littoral  
8 dune systems, coastal erosion and pollution (Snoussi et al. 2008; Viles and Spencer 2014).  
9 Marine submersion events, caused by storm surges and tsunamis, represent an additional  
10 pressure to these settings. These extreme events are today among the costliest natural disasters  
11 in terms of economic and human damage. In 2004, the Sumatra tsunami killed 165,708 people  
12 in Indonesia and caused economic losses estimated at US\$ 4.46 billion (EM-DAT Public). In  
13 2005, the United States suffered an estimated US\$ 125 billion in economic losses from  
14 Hurricane Katrina, as well as the deaths of 1,833 people (EM-DAT Public). The projected fast  
15 increase in coastal populations might expose 75% of the world's population to ocean-related  
16 hazards by the year 2025 (World Ocean Network in Finkl and Makowski 2019). Projections  
17 estimate that global (annual) losses from coastal flooding will increase from US\$ 6 billion in  
18 2005 to US\$ 52 billion in 2050 (Hallegatte et al. 2013).

19 The impact of storm surges and tsunamis on the Moroccan coasts will probably increase in the  
20 future. Firstly, because of the expected sea-level rise due to climate change (Li et al. 2018;  
21 Nagai et al. 2020). The latest IPCC report predicts a 2.5 m rise in mean sea level by 2100 for  
22 the RCP 8.5 scenario (Pachauri et al. 2014; Pörtner et al. 2019). With this, marine submersion  
23 events that are considered minor today will probably become more numerous and destructive  
24 in the future. Secondly, there is a strong demographic and economic growth observed on the  
25 Moroccan coastline. The urbanisation process has accelerated since Morocco's independence  
26 in 1965, with the development of large coastal urban areas, such as Casablanca, Tanger, Rabat,  
27 Kenitra, Safi, Agadir and Dakhla. The city of Casablanca, which in 1951 had about 683,000  
28 inhabitants, was home to 3.36 million inhabitants in 2014 (Haut Commissariat au Plan 2014).  
29 The city of Rabat, which had no more than 50,000 inhabitants at the beginning of the XX  
30 century, saw its population triple in 1951, with 203,000 inhabitants, to reach 577,827  
31 inhabitants in 2014 (Haut Commissariat au Plan 2014). The Moroccan coastline is also a  
32 structuring pole of the Moroccan economy. It brings together most of the tourist and industrial

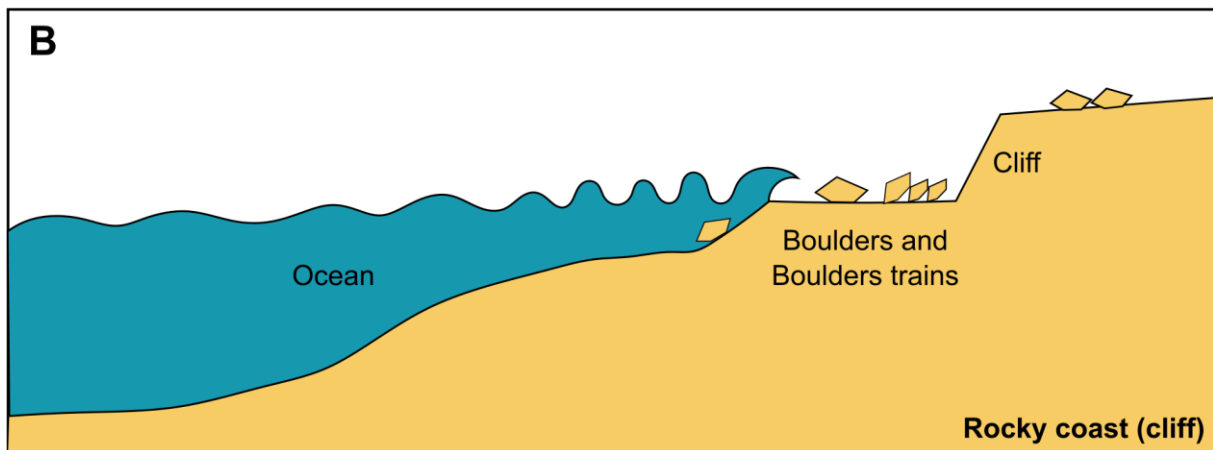
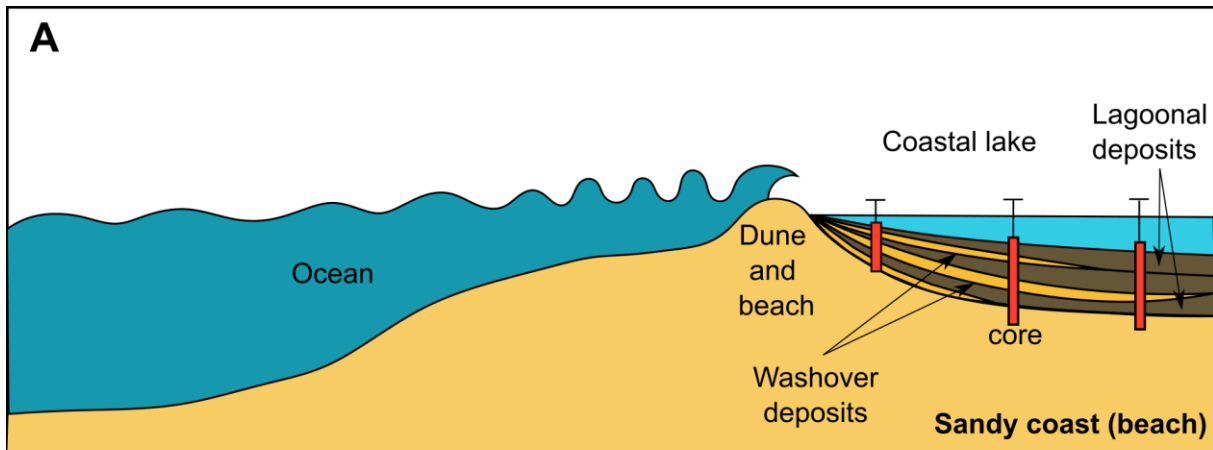
1 activities. The country's main port infrastructures are located in Tangier-Med, Casablanca,  
2 Mohammedia, Jorf-Lasfar and Agadir. There are also specific strategic infrastructures, such as  
3 the two large phosphate complexes of Jorf-Lasfar and Safi, as well as energy production plants,  
4 located in Jorf-Lasfar (2,016 Mw), Safi (1,386 MW) and Tahaddart (400 MW).

5 The current state of knowledge on Moroccan marine submersion events is based mainly on rare  
6 textual and instrumental records, which are insufficient to decipher the behaviour of these low-  
7 frequency, but high-impact events (Raji et al. 2015). Over the last 10 years, several coastal sites  
8 were investigated for sedimentary traces left by marine submersions, in the hope of dating them  
9 and filling the information gap regarding these natural hazards. Multiple sites with sedimentary  
10 evidences of these events were identified along the Moroccan coasts, in the form of boulders  
11 (Medina et al. 2011) and fine-grained sediments (typically sand-sized) (Mhammdi et al. 2015;  
12 Raji et al. 2015; El Talibi et al. 2016; Khalfaoui et al. 2020). Despite this effort, the number of  
13 studies is still low compared to the nearby Iberian coasts, which are confronted with the same  
14 natural disasters.

15 This work synthesizes and reviews the main methods and outcomes of all studies conducted on  
16 marine submersion deposits along the Moroccan coasts, in terms of geographic distribution,  
17 types of the sedimentary record, and proxies used to identify them. The study also proposes  
18 some recommendations for future research projects on this topic along the Moroccan coasts.

## 19 **2. Marine submersion deposits: identification proxies**

20 The study of marine submersion events using coastal sediments contributes to the extension of  
21 tsunami and storm surge catalogues beyond the historical record. In coastal low-energy  
22 environments, such as lagoons and coastal lakes, these events are preserved in the form of fine-  
23 grained deposits, also known as washover deposits (Dezileau et al. 2016; Baumann et al. 2017;  
24 Pouzet and Maanan 2020) (Fig. 1a). Along rocky shores, traces of storms and tsunamis are  
25 conserved in the form of boulder deposits (Paris et al. 2011; Terry et al. 2013) (Fig. 1b). We  
26 will present in this section an overview of some proxies used to study these two types of  
27 deposits. In the part dedicated to fine-grained deposits, we will focus on the sedimentological,  
28 geochemical and micropaleontological (benthic foraminifera) criteria since they are the most  
29 used along the Moroccan coasts. More details about the proxies applied to locate these onshore  
30 deposits can be found in Engel et al. (2020).



1

2 **Fig. 1** Marine submersion events landfall and deposits along sandy shores (a) and rocky coasts (b)

3 **2.1. Fine-grained deposits**

4 **2.1.1. Sedimentology**

5 Generally, protected coastal environments are dominated by fine-grained sediments, allowing  
 6 sandy sediments, deposited during marine submersion events, to create a grain-size anomaly in  
 7 the local stratigraphy (Figs. 1a and 2). When investigating cores or trenches from these  
 8 environments, it is possible to witness this abrupt change in grain size with a naked eye (Morton  
 9 et al. 2007). Sometimes, they present themselves as a single bed and sometimes they are  
 10 constructed from multiple beds, which illustrates several sedimentary phases of the same  
 11 submersion event. In their investigations of tsunami deposits placed by the second Storegga  
 12 landslide in Scotland, Shi et al. (1991) noted that these deposits were arranged in several  
 13 normally graded sandy layers. According to these authors, the Storegga landslide caused several  
 14 tsunami waves, which resulted in this type of multi-bed deposits. The normal grading is a  
 15 product of a gradual decrease of the wave energy during submersion (e.g. Shi et al. 1991;  
 16 Morton et al. 2007). Reverse grading can also be observed, but it is rare (Morton et al. 2007;  
 17 Choowong et al. 2008).

1 Sedimentary structures such as rip-up clasts and mud drapes can also be found in washover  
2 deposits (e.g. Dawson 1994; Moore et al. 1994; Goff et al. 2001). Rip-up clasts are generally  
3 positioned at the base of these deposits. Morton et al. (2007) and Jaffe et al. (2008) showed that  
4 cyclone deposits tend to not exhibit rip-up clasts due to the turbulence and prolonged vigorous  
5 agitation of storm waves, which breaks up and disperses clasts. However, Phantuwongraj et al.  
6 (2013) documented the presence of such structures at the base of a storm deposit in Laem  
7 Talumphuk, Thailand. It is worth mentioning that the deposit base may also contain imbricated  
8 gravels and shells that indicate the direction of the currents and waves responsible for their  
9 deposition (Goff et al. 2001). Mud drapes are layers of fine, organic-rich sediments that cap  
10 marine submersion deposits (Scheffers 2015). When sea waves reach their maximum  
11 penetration distances, and their velocities are weak, the hydrodynamic conditions are ideal for  
12 the sedimentation of these fine layers (Dawson 2000; Scheffers 2015).

13 On a cross-shore transect, the thickness of storm surge or tsunami deposits generally decreases  
14 with distance from the coastline. The inland penetration distance depends on the wave energy,  
15 the local topography (slope) and the roughness of the ground (Sato et al. 1995). The inland  
16 penetration limit of washover deposits is one of the criteria used to differentiate between storm  
17 surge and tsunami deposits in the same stratigraphic sequence. With the same wave heights,  
18 tsunami deposits can penetrate further inland than storm surge deposits because of their long  
19 wavelengths (Costa and Andrade 2020). The continuity of the depositional process is also a  
20 factor that is not always present. Deposits can be discontinuous due to topographic variations  
21 and post-depositional processes (mainly erosion) (Spiske et al. 2019).

22 Spiske et al. (2019) synthesised a set of natural and anthropogenic post-depositional processes,  
23 affecting tsunami deposits in arid environments. The natural post-depositional processes, which  
24 may occur simultaneously or individually, are erosion, compaction and bioturbation.  
25 Anthropogenic post-depositional processes are especially observed in urbanised coastal areas  
26 and are related to human activities after each disaster. For instance, in Peru, residents of areas  
27 affected by the Pisco-Paracas tsunami (2007) used the sand left by the waves to make cement  
28 to rebuild buildings damaged by the event (Spiske et al. 2013).



1

2 **Fig. 2** Photos before and after Hurricane Sandy (2012) opened a breach on Fire Island, and created a washover deposit behind the dune barrier  
3 (USGS Public Domain)

#### 4 2.1.2. Geochemistry

5 Before the 2004 tsunami, geochemistry was not usually used to analyse marine submersion  
6 deposits. This was due to the lack of geochemical expertise of the scientists working on the  
7 subject at the time (mostly sedimentologists), or because they believed that geochemistry was  
8 not necessary to demonstrate the marine source of these sediments and that this could be  
9 verified by microfossil analysis (Chagué 2020). After the 2004 event, geochemists started to  
10 work on recent tsunami deposits, especially the pore water part, to assess the environmental  
11 impact of tsunami waves on coastal resources. The results of these studies highlighted the  
12 problem of salinisation of agricultural land and drinking water resources (Szczuciński et al.  
13 2005, 2007), which is related to the high concentration of sea water with salt ions ( $\text{Na}^+$ ,  $\text{K}^+$ ,  $\text{Cl}^-$   
14 ,  $\text{Ca}^{2+}$  and  $\text{Mg}^{2+}$ ). Moreover, geochemists also noticed that extreme waves are capable of  
15 transporting contaminant-rich marine sediments in urbanised coastal areas. Sujatha et al. (2008)  
16 analysed the geochemistry of sediments collected three weeks after the 2004 tsunami in the  
17 Nagapattinam district of India, and the results showed that these deposits were richer in  
18 pollutants (metallic trace elements, phosphates, nitrates, etc.) compared to sediments collected  
19 at the same site during previous studies.

20 Geochemistry allows also the identification of marine submersion deposits through their  
21 mineralogical composition. Storm surge and tsunami deposits usually have a geochemical  
22 signature that is similar to coastal sandy sediments. The detection of calcium (Ca), strontium

1 (Sr) and magnesium (Mg) indicates the presence of biogenic carbonates in the sediment (e.g.,  
2 bivalves, gastropods, foraminifera, diatoms and ostracods) (Croudace and Rothwell 2015).  
3 Titanium (Ti), zirconium (Zr) and iron (Fe) can be associated with heavy minerals (Chagué-  
4 Goff 2010; Chagué-goff et al. 2011). Silicon (Si) is used to trace silicate minerals, such as quartz  
5 (Cuven et al. 2013; Yu et al. 2016). However, the use of this proxy requires a geochemical  
6 mapping of all sediment sources (marine and continental) arriving to the surveyed area. The  
7 geochemical signature of marine submersion deposits remains site-specific and highly  
8 dependent on regional geology (Dezileau et al. 2011; Sabatier et al. 2012; Degeai et al. 2015).

9 Post-depositional processes can alter the initial geochemical signature of marine submersion  
10 deposits. Since the work of Minoura et al. (1994), the chemistry of pore water has been little  
11 used to search for paleo deposits of storms and tsunamis (Chagué 2020). For instance, the  
12 preservation of salt ions in these deposits is conditioned by the nature of the sediment, the  
13 drainage processes (lateral and vertical) and the local climatic conditions (Chagué-Goff et al.  
14 2017). They can rapidly be diluted with precipitation and surface and/or groundwater  
15 movements. On the Indonesian coast of the Andaman Sea, Szczuciński et al. (2007) conducted  
16 annual monitoring of the salinity of sandy sediments deposited by the 2004 tsunami. The salt  
17 content in these deposits decreased considerably after the first rainy season, returning a few  
18 years after to its pre-tsunami level (Szczuciński et al. 2007). Fine sediments enriched with  
19 organic matter (OM) can retain salt ions over a long time. The latter can interact with the OM  
20 and take on an organic form, which allows them to be preserved for hundreds or even thousands  
21 of years (Biester et al. 2004; Shinozaki et al. 2016). In sedimentary sequences collected from  
22 the Petit Bog in Canada, Chagué-Goff and Fyfe (1996) detected several levels that were rich in  
23 halogen elements (Cl, I and Br), which would correspond to past marine submersion events.  
24 For the mineral part of the sediment, diagenetic and redox processes, linked to surface and  
25 groundwater circulation, could lead to the dissolution, mobilisation or precipitation of new  
26 chemical compounds (Chagué-Goff 2010; Donnelly et al. 2017). Despite this, the sediment  
27 geochemical signature, related to its mineral part, is less sensitive to post-depositional  
28 transformations, compared to sediment pore water. Chagué-Goff et al. (2012) showed that  
29 sandy deposits from the 2011 Tohoku-Oki tsunami and Jogan 869 CE had the same mineral  
30 geochemical signature (high Sr and Rb concentrations compared to the background  
31 sedimentation), reflecting the same sediment source for both events.



### 2.1.3. Benthic foraminifera

Due to their small size, high abundance and fossilisable tests, foraminifera are considered as good stratigraphic, palaeoecological and palaeoenvironmental indicators (Alfred R. Loeblich and Tappaan 1988; Hayward et al. 1999; Sen Gupta 2003). Benthic foraminifera assemblages in marine submersion deposits can indicate the source of the sediment from which they were transported (i.e., depth and distance) and the hydrodynamic characteristics of the waves responsible for their deposition (flow velocity and turbidity) (Mamo et al. 2009). In low-energy coastal environments, Mamo et al. (2009) synthesised a set of criteria for identifying marine submersion deposits using benthic foraminifera. These criteria include: (i) a change in assemblage composition compared to background sedimentation (e.g., a continental shelf species in a lagoon or estuarine environment) (Hindson et al. 1996; Hindson and Andrade 1999; Hawkes et al. 2007); (ii) a change in population numbers (Cundy et al. 2000; Hawkes et al. 2007; Kortekaas and Dawson 2007); (iii) a change in test size or juvenile/adult ratios (Guilbault et al. 1996); (vi) a change in the taphonomic character of tests (Hindson and Andrade 1999; Hawkes et al. 2007). On the Kenyan coast, Bahlburg and Weiss (2007) observed, in sediments deposited by the 2004 tsunami, a high abundance of benthic species normally living on the continental shelf at depths of less than 30 m (e.g. *Quinqueloculina* sp. and *Spiroloculina* sp.), and depths of 80 m (e.g. *Amphistegina lessonii* d'Orbigny, 1826). In sediments deposited by the 2004 tsunami on the Thai and Malaysian coasts, Hawkes et al. (2007) were able to differentiate the uprush deposit, characterised by offshore radiolarians, from the backwash deposit where remobilised mangrove foraminifera were present.

Differentiating between storm and tsunami deposits using foraminifera is a complicated task (Kortekaas and Dawson 2007). One might expect storm deposits to be composed of sedimentary material from the nearshore, with a taxonomy representative of these environments. Tsunami deposits would, instead, be composed of a wide range of sediments from the inner shelf to continental debris (Switzer and Jones 2008). Like geochemistry, the use of benthic foraminifera to trace the source of storm surge/tsunami sediments necessitates calibration by the study of their current ecological habitat using surface sediments (Pilarczyk et al. 2014). The study of surface foraminiferal assemblages helps elucidate taphonomic processes and refine paleoecological interpretations (Pilarczyk et al. 2014). However, post-depositional processes can affect the foraminiferal assemblage present in marine submersion deposits (Pilarczyk et al. 2014). For example, foraminifera with calcareous tests can have a low preservation potential. In deposits emplaced by the 2004 tsunami, and collected 4 years after the event, Yawsangratt

1 et al. (2012) found evidence of intense dissolution of calcareous foraminiferal tests. These  
2 taphonomic problems can be overcome using ancient foraminiferal DNA; a new approach that  
3 aims to identify the species of foraminifera present in sediment through their nucleic acids  
4 (Szczuciński et al. 2016).

#### 5 2.1.4. Age-estimation

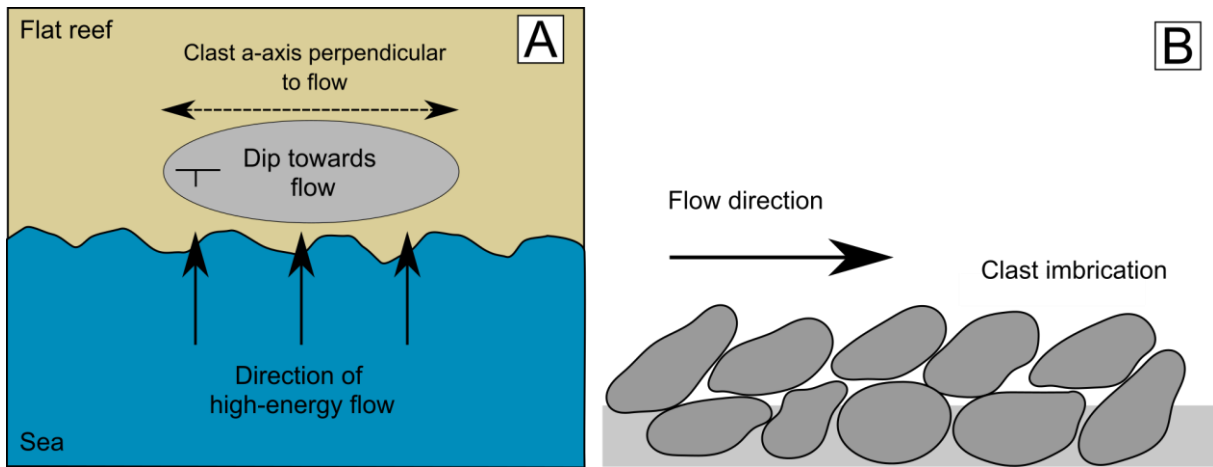
6 Marine submersion deposits are frequently dated using radiocarbon determination. It could be  
7 done on different types of carbon dating samples, such as animals, wood, plants and shells,  
8 extracted from the targeted deposit itself or the sediments in contact with it (Kelsey and Witter  
9 2020). On the one hand, if the carbon samples are extracted directly from the marine submersion  
10 deposit, duplicates are needed in this case to estimate its age, since it is possible to encounter  
11 remobilised carbon samples. In general, the most recent  $^{14}\text{C}$  age is the one that should be taken  
12 into account, and represent the maximum age of the deposit. On the other hand, if the carbon  
13 samples are retrieved from the horizons below and above the suspected storm or tsunami  
14 deposit, the probability of these samples being remobilised is low. They will provide both  
15 maximum and minimum limiting ages for the deposit. It is important to recognize and document  
16 the context of the samples relative to the deposit, for a better interpretation of the  $\text{C}^{14}$  ages.

17 Marine submersion deposits have been dated also using optically stimulated luminescence  
18 (OSL), which is an alternative to radiocarbon dating (Brill and Tamura 2020). OSL offers  
19 multiple advances compared to radiocarbon dating. Firstly, it provides robust ages for periods  
20 between a few years and several hundred thousand years (the entire Holocene and Pleistocene)  
21 (Ballarini et al. 2003; Walker 2005). Secondly, unlike radiocarbon dating, the presence of  
22 datable materials in tsunami or storm deposits is not an issue for OSL, since the dating is based  
23 on the sediment itself.

#### 24 2.2. Boulder deposits

25 Marine submersion events also have a physical impact on rocky coasts through the deposition  
26 of boulders (Fig. 1b). This type of deposit has been observed in different types of rocky coasts:  
27 cliff tops (Cox et al. 2019), rocky flats (Mhammdi et al. 2008) and coral reefs (Goto et al. 2010).  
28 Extreme wave action in such environments leads to the detachment and transport of boulders  
29 (of various sizes) inland. The arrangement of the boulders can take different forms: isolated  
30 blocks, clusters and/or nested, parallel to the coastline (Scardino et al. 2020). Examples of  
31 boulder deposits have been reported in several coastal areas around the world: Morocco  
32 (Medina et al. 2011), France (Regnaud et al. 2010), Japan (Goto et al. 2010), Algeria (Maouche

1 et al. 2009), Chile (Abad et al. 2020), Scotland (Hall et al. 2010; Scheffers et al. 2010), Hawaii  
2 (Noormets et al. 2002; Richmond et al. 2011) and Taiwan (Ota et al. 2015).



3  
4 **Fig. 3** (a) Cross-section of a boulder deposit in nested form, the direction of dip of the boulders is towards the source of the current. b) drawing  
5 showing an aerial view of a boulder deposit. The long axis is parallel to the direction of the flow. The boulder dips toward the source of the  
6 stream (redraw from Nichols (1999) in Terry et al. (2013))

7 Boulder deposits allow the estimation of a set of parameters that characterise the waves  
8 responsible for their emplacement, in terms of height, period, direction and propagation speed  
9 (Paris et al. 2010). The direction of propagation can be estimated through the orientation of the  
10 main axis of the boulders (the longest axis), which is generally perpendicular to the current  
11 (Nichols 2009) (Fig. 3a). Boulders in nested position dip in general towards the source of the  
12 current (Nichols 2009) (Fig. 3b). Goto et al. (2010) studied a boulder field emplaced by the  
13 2004 tsunami in the intertidal zone of Pakarang Head, Thailand. They found that the majority  
14 of boulders in these fields had the long axis oriented N-S, which corresponds to an E-W wave  
15 propagation direction, similar to the one obtained by modelling (Goto et al. 2010).  
16 Hydrodynamic equations were developed to estimate the energy required for the waves to  
17 transport the boulders, based on their physical characteristics (diameter, volume, weight and  
18 distance from the source) (Nandasena 2020; Cox et al. 2020).

19 Two approaches are proposed in the literature to date boulder deposits. The first one concerns  
20 relatively recent deposits and consists of analysing a set of photos, aerial images and high-  
21 resolution satellite images, taken on different dates for the same coastal area (Goto et al. 2011).  
22 This makes it possible to track the movement of existing boulders and to identify the  
23 emplacement of new ones. For older deposits, it is necessary to use classical dating methods.  
24  $^{14}\text{C}$  measurements from organisms attached to boulders can indicate their ages, assuming that  
25 these organisms died at the time of boulder detachment (Hall et al. 2006; Costa et al. 2011).  
26 Boulders containing corals can be dated by electron spin resonance (Scheffers and Kinis 2014).

1 Other studies use lichen coverage on boulders to estimate the age of emplacement (Matthews  
2 2012).

### 3 **3. Sources of storm surges and tsunamis along the Moroccan coasts**

4 Morocco is located in the northwesternmost part of Africa, with around 3500 kilometres of  
5 coastlines (500 km on the Mediterranean Sea and 3000 km on the Atlantic Ocean). The waves  
6 reaching the Atlantic coast are created by westerly winds travelling across the North Atlantic  
7 Ocean (Charrouf, 1991). They are not uniform but they show a general direction between WNW  
8 and N, with heights (Hs) between 0.5 and 3 m and periods (Ts) around 9-13 seconds (Charrouf,  
9 1991). The tides on the Atlantic coast are mesotidal and semidiurnal.

10 On the Mediterranean coast, around 90% of the significant wave heights (Hs) are under 1.5 m  
11 and only 5% above 3 m (El Mrini et al., 2012). The dominant wave periods range between 5  
12 and 6 s (El Mrini et al., 2012). The most frequent directions are E and NE (El Mrini et al., 2012).  
13 The tides on the Mediterranean coast are microtidal and semidiurnal.

#### 14 **3.1. Storm surges**

15 During the winter season, North Atlantic extratropical cyclones generate strong westerly winds  
16 that can produce extreme swells to the Moroccan Atlantic coast. According to the standards of  
17 the Moroccan National Weather Service, a wave is considered dangerous when its height  
18 exceeds 3 metres on the Mediterranean sea and the Strait of Gibraltar, and 4 metres on the  
19 Atlantic ([Http://vigilance.marocmeteo.ma/](http://vigilance.marocmeteo.ma/)). These waves can be dangerous, especially during  
20 spring tides. More rarely, tropical cyclonic systems can reach the Moroccan coast. Examples  
21 include Vince (8 - 11 October 2005), Delta (22 - 30 November 2005) and Leslie (11 - 14  
22 October 2018) (Fig. 4). These cyclonic systems often reach the end of their life cycle on the  
23 Moroccan coasts (Mhammdi et al. 2020).

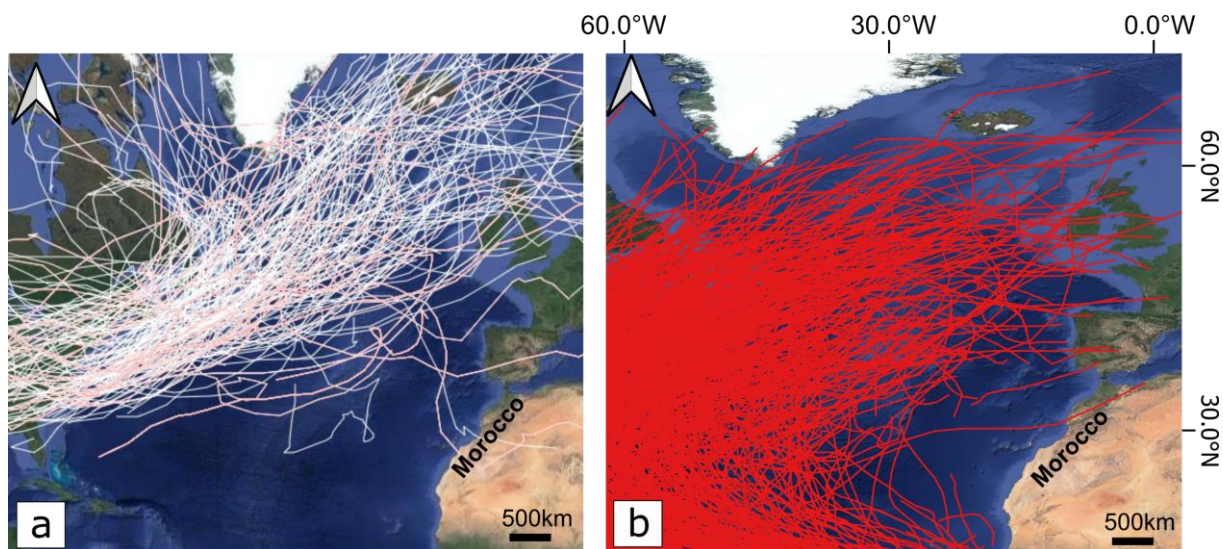


**Fig. 4** (a) Tracks of the 200 strongest extratropical storms in the North Atlantic between 1989 and 2009 (Atlas of Extratropical Storms, University of Reading, UK). (b) Tracks of historical tropical storms between 1850 and 2008 in the North Atlantic (NOAA database)

Mhammdi et al. (2020) synthesised the storm surge events that affected the Moroccan Atlantic coast between 1905 and 2018. This record brings together several tidal databases, such as Simonet and Tanguy (1956) and El Messaoudi et al. (2016). The work of Simonet and Tanguy (1956) contains wave data collected by the Earth Physics Department of the Cherifian Scientific Institute from several ports during the 1928-1952 CE period. El Messaoudi et al. (2016) present a list of some major storm events recorded by the National Weather Service between 1966 and 2014. This catalogue contains other events compiled by Minoubi et al. (2013) for the Safi region during the winters of 1948-1949, 1965-1966, 1973-1974 and 1985-1986 CE.

To our knowledge, there is no storm catalogue for the Mediterranean coast of Morocco. Raji (2014) mentioned some historical events in 1889 and 1941 CE that affected the Nador lagoon and breached its coastal barrier. Niazi (2007) also cited some historical storms that impacted the coast of Tetouan in 1963, 1989 and 1990. The event of 1963 completely destroyed the main jetty of the port of M'diq and was the result of strong eastern winds, known locally as "Chergui". Other local technical reports mention storms affecting the coast of Fnideq and M'diq in 1956 and 1957.

## 3.2. Tsunamis

### 3.2.1. Mediterranean coast

Tsunami events recorded in the western part of the Mediterranean Sea are less destructive compared to the Atlantic ones. Two areas were defined by Papadopoulos and Fokaefs (2005) as part of an intermediate tsunamigenic zone: (i) the Alboran Sea environment, characterized by the dominance of strike-slip fault systems and, (ii) the Tell Atlas belt, Northern Algeria,



1 characterized by a compressive type of deformation forming thrusts and folds (Figs. 5a and 5c).  
2 In the Alboran Sea, Álvarez-Gómez et al. (2011) identified twelve probable tsunamigenic  
3 seismic sources. The most dangerous source would be the Alboran Ridge fault system, which  
4 is capable of generating tsunami wave heights up to 1.5 m at the receiving shores (for water  
5 depths <80 m) in Spain and Morocco (Álvarez-Gómez et al. 2011). The seismic activity of the  
6 North Algerian Fold and Thrust Belt also represents a moderate tsunami source for the Iberian  
7 and North African coasts (Álvarez-Gómez et al. 2011). For the 1980 El Asnam earthquake, the  
8 maximal water heights were between 0.3–0.4 m, recorded at tide gauges between Cartagena  
9 and Alicante (South-Eastern Spain) (Roger et al. 2011). However, historical archives indicate  
10 the occurrence of multiple major tsunami events associated with  $M_w > 6$  earthquakes, such as  
11 1522, 1680, 1790 and 1804 CE (Kaabouben et al. 2009; Maramai et al. 2014).

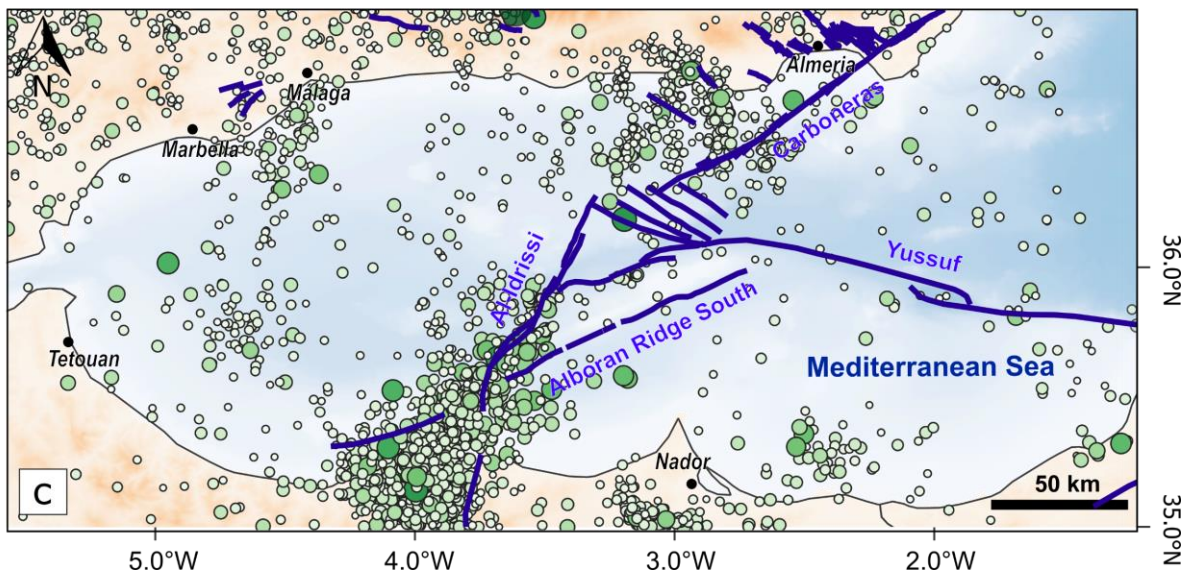
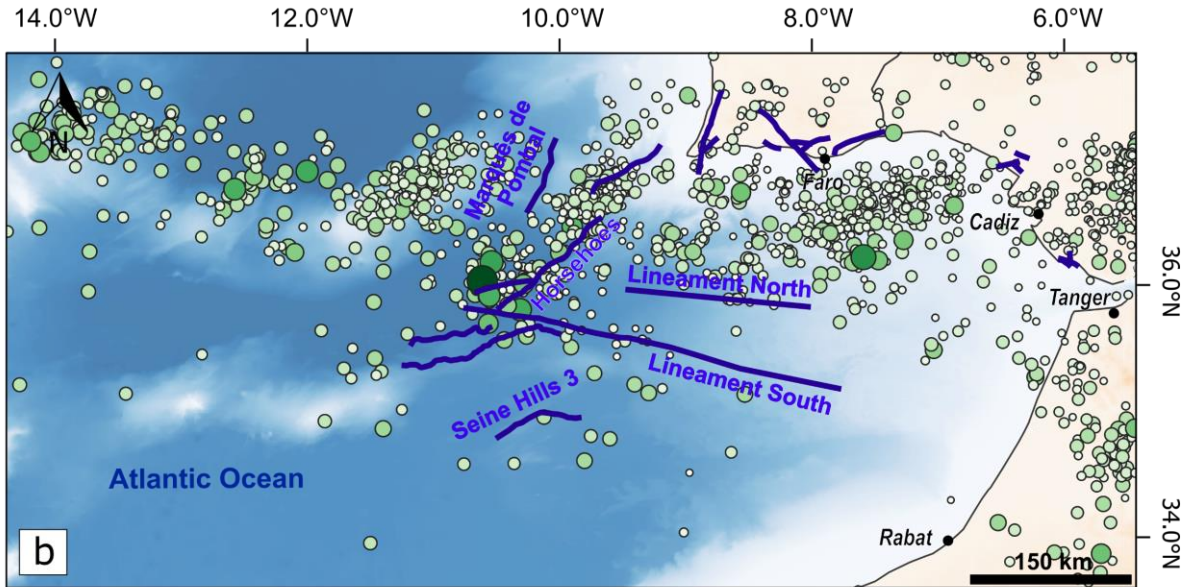
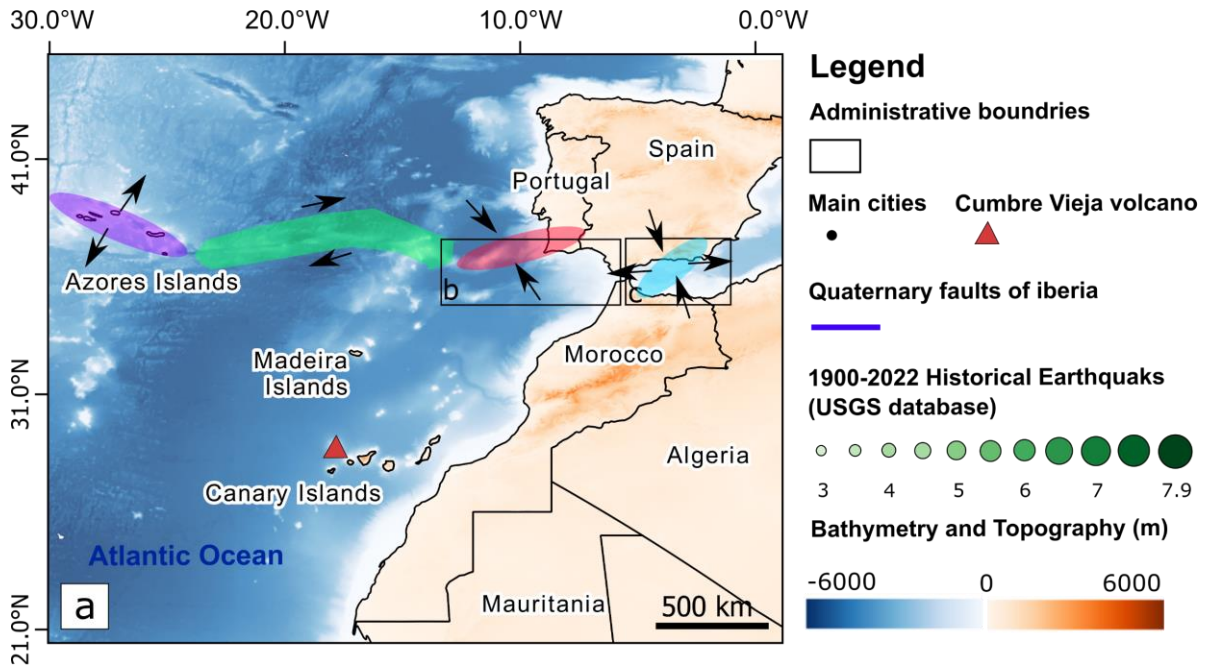
12 Recent studies reported that tsunami events in the Alboran basin could also be triggered by  
13 sedimentary instability processes affecting the seafloor surface. The development of  
14 exploration techniques has revealed the presence of numerous potentially tsunamigenic  
15 landslides on the seafloor surface, at the southern Alboran Ridge (Al-Borani landslide) (Macías  
16 et al. 2015), along the northern Alboran continental slope (Baraza Slide) (Casas et al. 2011),  
17 Along the northern Xauen–Tofino bank (Rodriguez et al. 2017) and northeastern seamounts  
18 (Alonso et al. 2014). Macías et al. (2015) simulated a possible tsunami generated by the Al-  
19 Borani submarine landslide and found out that it can produce tsunami waves with a maximal  
20 amplitude of 1 m at the Moroccan coastline (single landslide; water depths <80 m). Following  
21 the same approach, Rodriguez et al. (2017) showed that a submarine landslide similar to the  
22 one located Along the northern Xauen–Tofino banks, can produce a tsunami with an elevation  
23 of the order of 1 m at the Moroccan coast (similar to the Al-Borani landslide). The most  
24 dangerous characteristic of this tsunami is the short propagation time between the source and  
25 the Moroccan coastline, on the order of 13 min, which represents a major threat to cities like  
26 Al-Hoceima. Reicherter and Becker-Heidmann (2009) indicate that the 1522 Almeria  
27 earthquake may have generated a submarine landslide along its offshore segment, which  
28 probably produced a tsunami (with run-up between 1 and 3 m) well recorded in coastal  
29 sediments.

### 30 3.2.2. Atlantic coast

31 Most of the historical tsunamis that affected the Atlantic coast of Morocco were generated by  
32 submarine earthquakes, distributed along the western segment of the Eurasia-Nubia plate  
33 boundary, between the Azores archipelago and the Strait of Gibraltar (Figs. 5a and 5b). This

1 boundary is controlled by different tectonic structures with different regimes from the West to  
2 the East: (i) an extensional regime near the Azores archipelago; (ii) a lateral strike-slip regime  
3 along the Gloria Fault; and (iii) a compressional regime in the South West Iberian Margin  
4 (Serpelloni et al. 2007). Seismic tsunamis in the area are produced mainly by the Gloria fault  
5 and from the South West Iberian Margin (SWIM) (Luque et al. 2002; Baptista and Miranda  
6 2009). The latter is characterized by the presence of several tectonic active structures, such as  
7 the Marquês de Pombal, the Gorringe bank, the Horseshoe, and the Cadiz faults (Johnston,  
8 1996; Zitellini et al., 1999; Gràcia et al., 2003; Matias et al., 2005; Gutscher, 2006). The major  
9 historical events in the area include the 218-209 BC Lacus Lingustinus tsunami (Campos 1991),  
10 the 1 November 1755 Lisbon earthquake and tsunami ( $M_w \geq 8.5$ ) (Baptista and Miranda 2009),  
11 and the recent 28 February 1969 Horseshoe earthquake and tsunami ( $M_w$  7.9-8.0). The 1755  
12 CE Lisbon tsunami caused massive damage to the Iberian and Moroccan Atlantic coasts and  
13 remains the most destructive in the history of the European region (Baptista et al. 1998). The  
14 waves propagated to the eastern Lesser Antilles, Brazil and Newfoundland, Canada (Kozak et  
15 al. 2005; Roger et al. 2010; Biguenet et al. 2021).

16 The second source of tsunamis is the volcanic activity of some archipelagos located near  
17 Morocco (Canary, Azores and Cape Verde Islands). For example, studies reported that the  
18 explosion of the La Palma volcano in the Canary Islands could produce a slip of one of its flanks  
19 to the sea, which in turn will cause large tsunami waves (Abadie et al. 2012, 2020). One of the  
20 most remarkable tsunami events is that of the volcanic island of Fogo in Cape Verde. The  
21 eruption of this volcano, dated 70,000 years ago, caused its eastern flank to collapse into the  
22 sea, which is believed to have formed a gigantic sea wave of almost 300 metres in height  
23 (Ramalho et al. 2015). Boulders weighing 700 tonnes were found on Santiago Island, 650  
24 metres from the coast, between 150 and 200 metres above sea level (Ramalho et al. 2015).



1



1 **Fig. 5** (a) source of tsunamis on the Moroccan coasts. Major kinematics and tectonics features of the Nubia-Eurasia plate boundary between  
2 the Azores islands and Alboran sea are from Serpelloni et al. (2007): purple= extensional regimes in the Azores archipelago, green =  
3 transcurrent regime along Gloria fault, red = compressional regime in the South West Iberian Margin, cyan = transtensional regime the Alboran  
4 Sea. (b) main faults and historical earthquakes (1900-2022) in the Gulf of Cadiz. (c) main faults and historical earthquakes (1900-2022) in the  
5 Alboran sea. Historical earthquakes are from the NOAA database. Major quaternary faults of Iberia are from QAFI database (García-  
6 Mayordomo et al. 2012)

7 Far-field tsunami sources can also threaten the Moroccan Atlantic coast. On the other side of  
8 the Atlantic, these events can be caused by the Northwestern Atlantic Ocean Submarine  
9 Landslides, the Puerto Rico Trench, and the northern Cuba fold-and-thrust belt (ten Brink et al.  
10 2014; Costa et al. 2021). The 1929 CE Grand Banks earthquake in Canada triggered a tsunami  
11 that was instrumentally measured across the Atlantic Ocean to the coasts of Portugal and the  
12 Azores islands (Fine et al. 2005).

#### 13 **4. Geological evidence of past marine submersion events**

14 Despite the important work conducted so far on Moroccan coastal Quaternary deposits, few  
15 studies have been devoted to storm surge and tsunami deposits. Gigout (1957) reported the  
16 presence of isolated blocks along the coastal region of Rabat and connected their movement  
17 and overturning to storm surge events. The first work on marine high-energy deposits was the  
18 one conducted by Mhammdi et al. (2008), to re-examine the blocks mentioned by Gigout (1957)  
19 and to assess their potential relationship to the 1755 CE Lisbon tsunami. Table 1 synthesises  
20 the work done so far on marine submersion deposits along the Atlantic and Mediterranean  
21 coasts of Morocco between 2008 and 2022. The locations of these studies are presented in Fig.  
22 6.

1

2

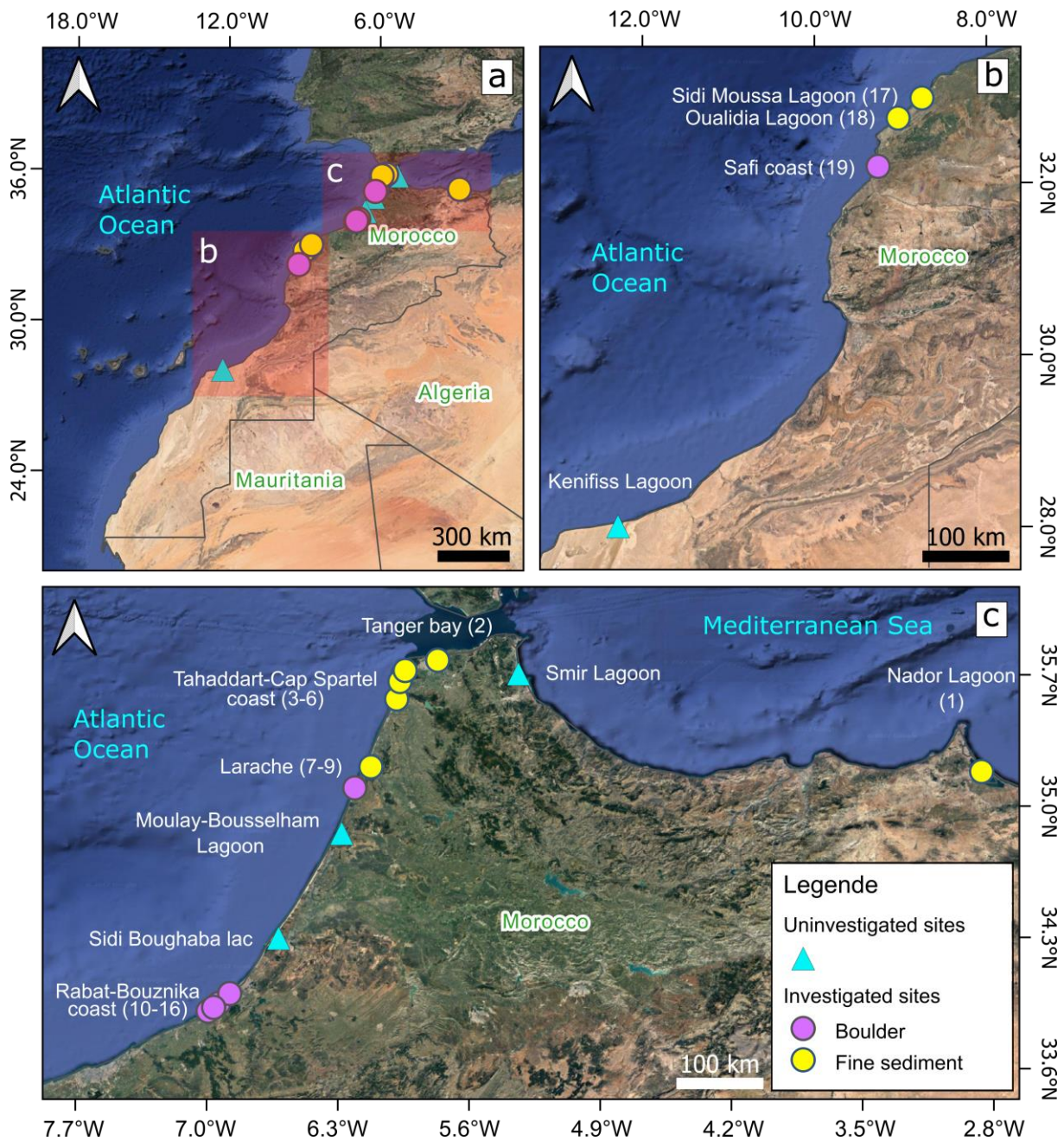
**Table 1** Summary of marine submersion deposits located on the Moroccan coasts. Geographic positions of the sites are in figure 6.

ID number	Location	Latitude/longitude	Type of deposit	Proxies used	Age (cal BP)	Selected references
1	Marchica Lagoon (Nador)	35° 09' 36" N 2° 50' 24" W	Fine sediment	Geochemistry Grain-size X-radiography Radiochronology ( <sup>14</sup> C, <sup>210</sup> Pb <sub>ex</sub> , <sup>137</sup> Cs) Macrofauna analysis Clay mineral analysis (XRD) Geophysics (high-resolution seismic)	61 160 428	Raji 2014; Raji et al. 2015, 2018
2	Tanger bay	35°46'42.55" N 5°46'5.57" W	Fine sediment	Grain-size Morphoscopy		Genet 2011
3	Tahaddart-Cap Spartel coast	35°34'15.22" N 5°59'9.94" W	Fine sediment	Grain-size Anisotropy of Magnetic Susceptibility Microfauna analysis		El Talibi 2016; El Talibi et al. 2016
4	Tahaddart-Cap Spartel coast	35°42'21.54"N 5°57'6.00"W	Fine sediment	Grain-size Quartz exoscopy Heavy mineral Microfauna analysis		El Talibi 2016; El Talibi et al. 2020
5	Tahaddart-Cap Spartel	35°39'52.04"N 5°58'5.74"W	Fine sediment	Grain-size Morphoscopy		Genet 2011
6	Tahaddart-Cap Spartel	35°34'15.22" N 5°59'9.94" W	Fine sediment	Grain-size Geochemistry Microfauna analysis (Benthic foraminifera) Organic matter content CaCO <sub>3</sub> content Radiochronology ( <sup>210</sup> Pb, <sup>137</sup> Cs and <sup>14</sup> C)	195 625 2700 3800	Khalfaoui et al. 2020; Khalfaoui 2021 Khalifaoui et al. (submitted to CSR)
7	Larache	35°10'37.62"N 6° 5'47.87"W	Fine sediment	Grain-size Magnetic Susceptibility (MS) CaCO <sub>3</sub> content		Mhammdi et al. 2015
8	Larache	35°5'50.00"N 6°12'33.00"W	Boulders			Medina et al. 2011

9	Larache	35° 8'39.63"N 6°11'18.83"W	Boulders			Sedrati et al. 2022
10	Rabat-Bouznika coast	33°54'25.24"N 6°59'30.95"W	Boulders	OSL-RSED	Inconclusive	Mhammdi et al. 2008; Medina et al. 2011; Belkhat et al. 2017; Chiguer and Medina 2019; Brill et al. 2021
11	Rabat-Bouznika coast	33°56'53.00"N 6°56'5.00"W	Boulders	OSL-RSED	Inconclusive	Mhammdi et al. 2008; Medina et al. 2011; Belkhat et al. 2017; Chiguer and Medina 2019; Brill et al. 2021
12	Rabat-Bouznika coast	34° 0'3.81"N 6°52'34.50"W	Boulders	OSL-RSED	Inconclusive	Mhammdi et al. 2008; Medina et al. 2011; Belkhat et al. 2017; Chiguer and Medina 2019; Brill et al. 2021
13	Rabat-Bouznika coast	33°55'37.77"N 6°57'42.94"W	Boulders	OSL-RSED	Inconclusive	Mhammdi et al. 2008; Medina et al. 2011; Belkhat et al. 2017; Chiguer and Medina 2019; Brill et al. 2021
14	Rabat-Bouznika coast	33° 48.596'N 7° 11.137'W	Boulders			Medina et al. 2018
15	Rabat-Bouznika coast	33°57'35.244" N 6°55'10.776" W	Fine sediment	Grain-size Radiochronology ( <sup>14</sup> C)	Inconclusive (estimated age between 9900 and 2200)	Chahid et al. 2016
			Boulders			Chahid et al. 2016
16	Rabat-Bouznika coast	33° 50.348'N 7° 6.644'W	Fine sediment	Grain-size Radiochronology ( <sup>14</sup> C)	Inconclusive (estimated age between 8000 and 4000)	Chahid et al. 2016
			Boulders			Chahid et al. 2016
17	Sidi Moussa lagoon	32°59'3.15"N 8°44'59.84"W	Fine sediment	Grain-size Organic matter content CaCO <sub>3</sub> content		Mellas 2012
			Boulders			Mellas 2012
18	Oualidia lagoon	32°45'1.14"N 9° 1'33.02"W	Fine sediment	Grain-size Organic matter content CaCO <sub>3</sub> content		Leorri et al. 2010; Lopes et al. 2010; Mellas 2012

<b>19</b>	Safi coast	32°11'18.77"N 9°15'30.70"W	Boulders			Theilen-Willige et al. 2013
-----------	------------	-------------------------------	----------	--	--	-----------------------------

1



2

3 **Fig. 6** Position of investigated and uninvestigated sites for marine submersion deposits along the Moroccan coasts. The numbers in brackets  
 4 correspond to the ID number in Table 1

#### 5 4.1. Mediterranean coast

##### 6 4.1.1. Marchica Lagoon (Nador)

7 The only work on marine extreme events along the Mediterranean coastline was conducted by  
 8 Raji et al. (2015) in the Marchica lagoon (Nador) (1 in Fig. 6c). In this study, sediment cores  
 9 were collected inside the lagoon following long-shore and cross-shore transects. Geochemical  
 10 and sedimentological analysis of the MC45 core showed the presence of three sandy levels, of

1 coastal origin, trapped within the lagoon's fine stratigraphy. Chronological data ( $^{14}\text{C}$ ,  $^{210}\text{Pb}_{\text{ex}}$   
2 and  $^{137}\text{Cs}$ ) placed these three events over the last 500 years. Based on local and regional  
3 historical records, Raji et al. (2015) associated these deposits with the storm of 1889 CE and  
4 the two tsunamis of 1522 CE and 1790 CE.

5 In terms of best practices, the work of Raji et al. (2015) is a good example to follow in the study  
6 of marine submersion deposits along the Moroccan coast. The multiproxy approach, based on  
7 grain-size analysis, XRF geochemistry and geophysics, increases the chances of identifying  
8 these types of deposits in low-energy coastal environments. The use of different radioisotopes  
9 ( $^{137}\text{Cs}$ ,  $^{210}\text{Pb}_{\text{ex}}$  and  $^{14}\text{C}$ ) refines the age of the storm surge or tsunami deposits. On the other  
10 hand, the combination of results from sedimentary archives and seismic is suitable to evaluate  
11 the maximum extension of the most intense marine submersion events over the whole lagoon  
12 (Raji et al. 2018).

## 1 4.2. Strait of Gibraltar

### 2 4.2.1. Tanger bay

3 A small coastal marsh in Tanger bay was one of the areas surveyed by Genet (2011) (2 in Fig.  
4 6c). It is a small coastal alluvial plain about 1 km long and 300 m wide, crossed by a small river  
5 called Oued Mlaleh. Five cores, with a length between 1 and 3 meters, were collected within  
6 the plain along a cross-shore transect. The records revealed the presence of a few levels of  
7 coastal sand trapped inside the fine estuarine stratigraphy (Fig. 7a). Genet (2011) believes that  
8 these deposits were emplaced by extreme marine events.

## 9 4.3. Atlantic coast

### 10 4.3.1. Tahaddart-Cap Spartel coast

11 The coastal section between Cape Spartel and the Tahaddart thermal power plant was  
12 prospected by Genet (2011) and El Talibi et al. (2020) (3-6 in Fig. 6c). This coastal section  
13 contains a few ponds and marshes, located behind a low dune ridge and seems to be favourable  
14 for the sedimentary record of marine submersion events. Genet (2011) conducted manual coring  
15 and trenching in the Boukhalef lagoon and the periphery of the Houara marsh. Trenches cleared  
16 in a construction site near Houara marsh revealed sandy levels interspersed in the local  
17 stratigraphy and resting discontinuously on a paleosol. The presence of rip-up clast and some  
18 mud-drapes, associated with bioclasts of marine origin, were all indicators of a marine high-  
19 energy deposit (Genet 2011). El Talibi et al. (2020) investigated the mouth of the Boukadou  
20 River, located north of Tahaddart. The study focused on three trenches, 20 to 30 cm long,  
21 oriented along a cross-shore transect. A sandy level was identified in all three trenches and rests  
22 discontinuously on a paleosol. The marine origin of this level was justified by its richness in  
23 marine bioclasts (foraminifera and molluscs), and by its grain size, which is similar to present-  
24 day beach sediments. The investigated deposit becomes thinner from the coast, reflecting a  
25 progressive decrease in the energy of the waves (El Talibi et al. 2020). The authors agreed on  
26 the 1755 CE event as a potential source of these high-energy deposits.

27 At the Tahaddart estuary, El Talibi et al. (2016) identified morphological and sedimentary  
28 evidences of an ancient marine submersion event between coastal dunes of Pleistocene age (3-  
29 6 in Fig. 6c). The interdune spaces were filled mainly with sediments eroded from the  
30 Pleistocene dunes during the submersion. The authors attempted to reconstruct the wave  
31 direction associated with the event using grain size and anisotropy of magnetic susceptibility  
32 measurements. The results showed two main directions: N91°-171° and N280°-325°, which



1 corresponded respectively to the uprush and backwash currents. Taking into consideration the  
2 different possible sources of tsunamis, the obtained wave directions were tentatively interpreted  
3 as a result of the Lisbon tsunami in 1755 CE. Wave heights were estimated to be between 6 and  
4 8 m for this event.

5 Not far from the site investigated by El Talibi et al. (2016), several sediment cores were  
6 collected in 2017 from the salt-marsh area (behind the coastal dunes) by Khalfaoui et al. (2020)  
7 and Khalfaoui (2021) (3-6 in Fig. 6c). The objective was to reconstruct the paleoenvironmental  
8 evolution of the Tahaddart lower estuary during the mid- to late Holocene and to identify  
9 possible records of ancient marine submersion events. These cores were examined using a  
10 multi-proxy approach, combining sedimentological (visual description; laser grain-size),  
11 geochemical (LOI, CaCO<sub>3</sub> and pXRF) and micropaleontological (benthic foraminifera)  
12 analyses, supported by <sup>210</sup>Pb, <sup>137</sup>Cs and <sup>14</sup>C time series data. This work revealed the first well-  
13 dated deposits of the 1755 CE tsunami on the Moroccan Atlantic coast (named SM1). Three  
14 older events, with a mean age of 625, 2700 and 3800 cal BP (named SM2, SM3 and SM4  
15 respectively), were also identified in the framework of this work, and correspond probably to  
16 some tsunami events, recorded in the Iberian Atlantic coast.

#### 17 4.3.2. Larache

18 Mhammdi et al. (2015) analysed a sediment core collected from the Loukkos estuary (CARLA-  
19 11) using multiple proxies, including grain size, magnetic susceptibility and carbon content (7-  
20 9 in Fig. 6c; Fig. 7b). The results revealed the presence of a 15 cm sandy level rich in marine  
21 shells trapped in fine estuarine sediments. Given the distance of the core from the shoreline (6  
22 km), the authors interpreted this sandy layer as a tsunami event. An estimated age, between  
23 5000 and 3000 BP, was given to this deposit based on chronological data provided by Carmona  
24 and Ruiz (2009) from fluvial terraces surrounding the CARLA-11 archive.

25 Medina et al. (2011) mentioned the presence of boulder deposits in the same area (7-9 in Fig.  
26 6c; Figs. 8a and 8b). They are small compared to the ones found by the same authors on the  
27 Rabat-Bouznika coast, with a respective volume and maximum weight of ~10.7 m<sup>3</sup> and ~23.5  
28 tons. These boulders are mostly leaning against the cliff in a nested position.

29 In the rocky shore platform of Laghdira (south of Larache city), Sedrati et al. (2022) used  
30 unmanned aerial vehicle (UAV)-based digital photogrammetry and SfM differential models to  
31 investigate the potential boulder transport and detachment triggered by a strong storm in 2019,  
32 and to identify possible boulder transport modes (7-9 in Fig. 6c). The authors reported the



1 detachment and mobilization of three boulders and the emplacement of a new one, as a result  
2 of the storm. The types of movements documented are sliding, saltation and boulders overturn  
3 with contrasting sizes and volumes.

#### 4 4.3.3. Rabat-Bouznika coast

5 On the Rabat-Bouznika coastline, two types of high-energy deposits have been identified:  
6 boulders and fine dune deposits (10-16 in Fig. 6c). Mhammdi et al. (2008) re-investigated the  
7 boulders recognised by Gigout (1959). A total of four sites were studied, namely Harhoura  
8 beach, Témara beach, Val d'Or beach and south of Skhirat beach. According to these authors,  
9 the boulders were detached from the active cliff during a high-energy marine event(s) and then  
10 transported over variable distances, from a few meters to 300 m. The shape of these boulders is  
11 generally flat, with a maximum length (axis A) of 9.8 m at Val d'Or. The weight of these  
12 structures is estimated between 4 and 100 tons. They can be found as single blocks, as a train  
13 of interlocking boulders or as a chaotic agglomerate. The study conducted by Medina et al.  
14 (2011) provides more quantitative results. It focused on the sites of Val d'Or, Harhoura and Cité  
15 Yacoub El Mansour. The direction of inclination and imbrication of the boulders was variable  
16 (N, NW and W). Their displacement distance reaches 150 m. According to hydrodynamic  
17 modelling, it is necessary to have waves with an amplitude of 5 to 11 m to move these boulders,  
18 which can be encountered in tsunami events (Medina et al., 2011).

19 Brill et al. (2021) tried to date some of the Rabat-Bouznika boulders using optically stimulated  
20 luminescence rock surface exposure dating measurements (OSL-RSED) (10-16 in Fig. 6c; Fig.  
21 8c). The results revealed large variability in the age of the boulders and were considered not  
22 conclusive. According to these authors, the variability was related to the low amounts of quartz  
23 and potassium feldspar in the source rock of the boulders, and to post-depositional erosion  
24 affecting some blocks. The major finding of this work was that the tsunami of 1755 CE was not  
25 the only event responsible for the deposition of these boulders, and that storm surge events have  
26 also played an important role in this process. According to these authors, storm surge events  
27 moved or reversed boulders with a weight greater than 24 tons. These results were in agreement  
28 with Medina et al. (2018) who noticed also the displacement of a large boulder (33 tons) in  
29 Dohemy beach (near Bouznika) during the winters of 2011-2012.

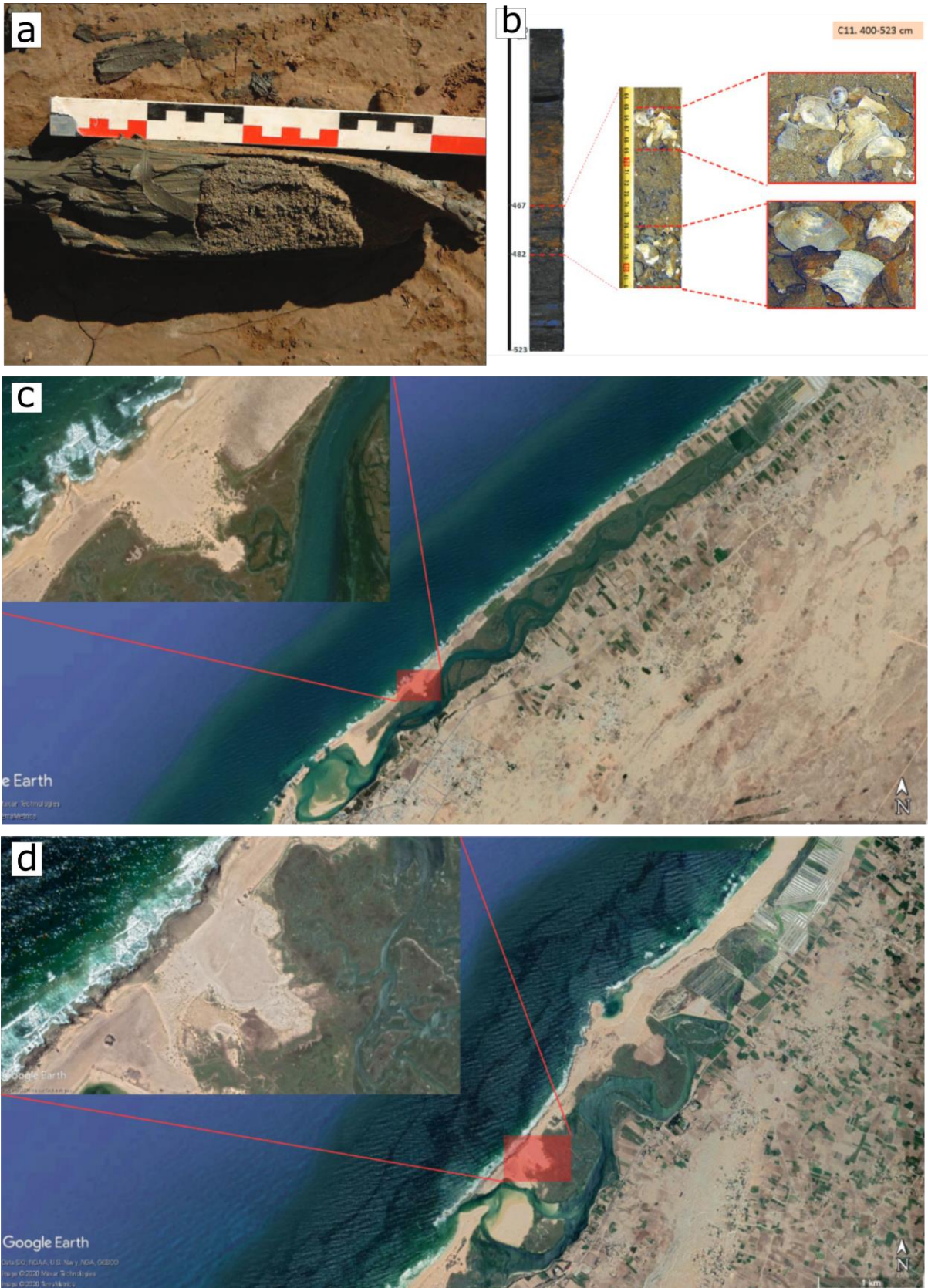
30 Another work carried out by Chahid et al. (2016) in the Rabat-Bouznika area revealed the  
31 presence of other high-energy deposits (10-16 in Fig. 6c). These authors studied two  
32 stratigraphic sections cleared in two Holocene dune formations located in Harhoura and Skhirat.

1 The Harhoura section is positioned 20 m from the shoreline and is about 2 m thick. It consists  
2 of a succession of massive sandy deposits, composed of poorly classified sands and shells,  
3 similar to the sand deposited on the present beach. These levels, interpreted by the authors as  
4 high energy levels, are separated by horizons of young soils rich in gastropods and marine  
5 shells. This Harhoura section is also characterized by the presence of several clusters of  
6 boulders, which reinforces the event-driven aspect of the deposits that form this section. <sup>14</sup>C  
7 dating, performed on this section, places these high-energy deposits between 9900 and 2200 cal  
8 BP (Chahid et al. 2016). The second section is located in Skhirat, north of the mouth of the  
9 Cherrat river. The authors describe a dune belt formed by a succession of poorly consolidated  
10 calcarenites, emplaced probably by high-energy marine events. The sedimentary structure and  
11 texture of these sandy levels (bedding, load figures, shell beds and pebbles) are related to wave  
12 breaking and washover deposition (Chahid et al. 2016). The construction of this second section  
13 was estimated to be between 8000 and 4000 cal BP (Chahid et al., 2016). The presence of  
14 cemented calcarenite boulders on their surfaces is another indicator of high-energy event driven  
15 deposition (Chahid et al. 2016).

#### 16 4.3.4. Oualidia and Sidi Moussa lagoons

17 Leorri et al. (2010) and Mellas (2012) studied two washover deposits, as well as boulders  
18 located in the lagoon of Oualidia and Sidi Moussa (17 and 18 in Fig. 6b). The washover deposit  
19 in the Oualidia lagoon is located about 900 m north of the main channel (Fig. 7c). It is about  
20 200 m wide by 120-130 m long. Two cores and a trench were performed by Mellas (2012) in  
21 the washover to characterize it in depth. The extracted sequences are constructed from coarse  
22 sands rich in shell debris, as well as a few marine benthic foraminiferas, like *Cibicides*  
23 *lobatulus*, *Ammonia beccarii*, and *Elphidium crispum*. This deposit lays discontinuously on  
24 autochthonous lagoonal fine sediments. Chronologically, no dating has been performed on this  
25 washover deposit. The Sidi Moussa washover is located about 1 km north of the main pass. It  
26 is 150 m long by 130 m wide (Mellas 2012) (Fig. 7d). This deposit was also studied at depth  
27 through coring. The sedimentological and micropaleontological results show the presence of a  
28 succession of shell-like coarse sandy levels of variable thickness (10 to 110 cm). These deposits  
29 are underlain by muddy lagoonal sediments. According to Mellas (2012), these deposits are  
30 probably the result of several marine high-energy waves (tsunamis or storm surges). Several  
31 isolated or clustered boulders (about 20) were also reported in this lagoon near the washover  
32 deposit. They were distributed parallel to the coastline and characterized by their elongated

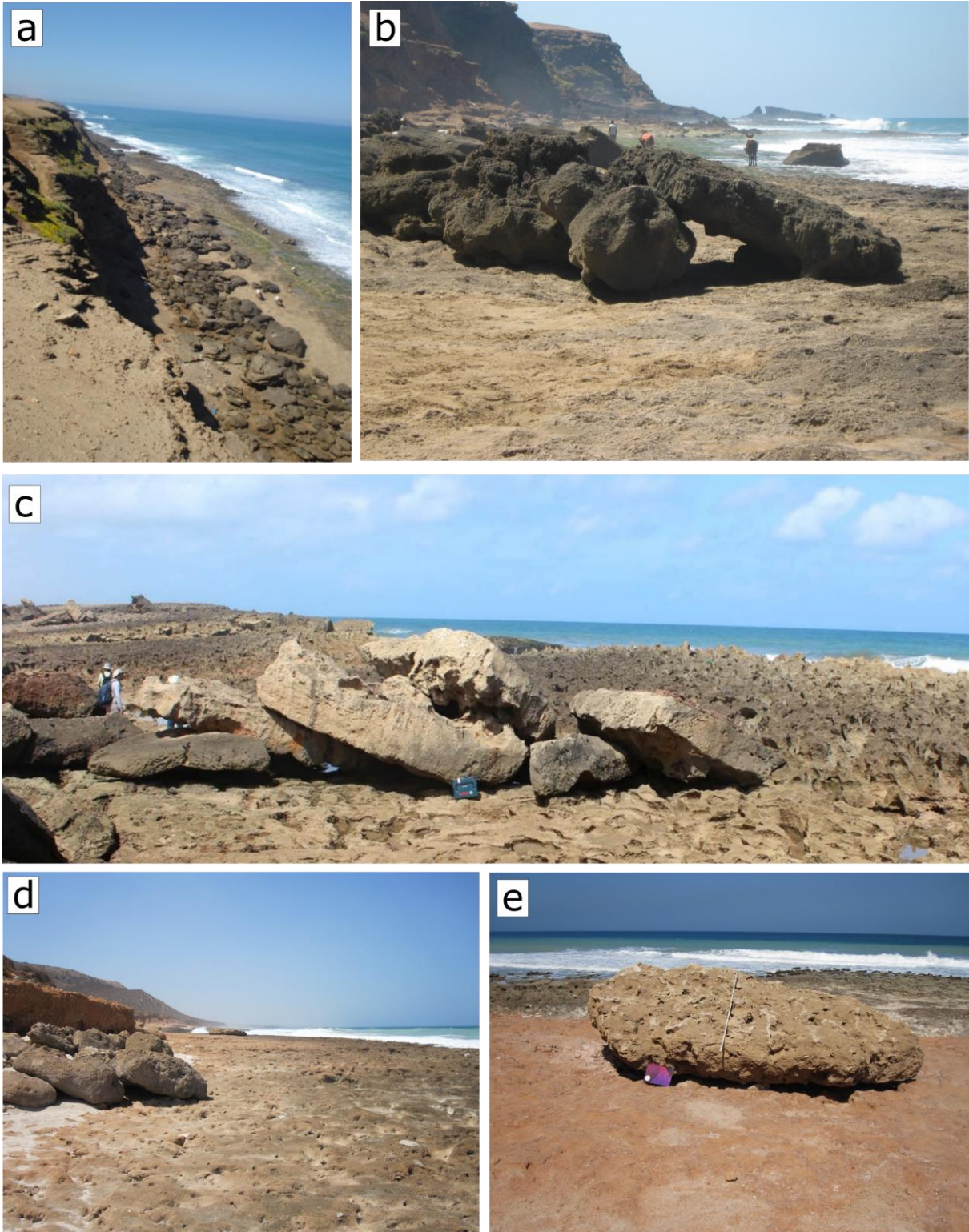
- 1 shapes with a major axis of 0.65-3.5 m (A-axis). No chronological data was provided for the
- 2 washover and the boulders.



1  
2  
3  
4  
5

**Fig. 7** Mosaic of field photos of fine-grained deposits along the Moroccan coastlines. (a) Tsunami deposit recovered with an auger from a small marsh in the bay of Tanger (Genet, 2011). (b) Tsunami-related sediments in the Carla-11 core at 6 km from the mouth of Loukkos river. 15 cm level showing more or less well-preserved sands and shells intercalated in wetland mud sediments (Mhammdi et al., 2015). (c) Washover of Oualidia lagoon (Google Earth). (d) Washover of Sidi Moussa lagoon (Google Earth)





1

2 **Fig. 8** Mosaic of filed photos of boulder deposits along the Moroccan coastlines. (a, b) Panoramic photos of the Larache boulder field. (c)  
 3 Seven interlocking boulder deposits aligned along the coast of Rabat and were probably deposited by the 1755 Lisbon tsunami (photo courtesy  
 4 of Simon Matthias May). (d,e) Panoramic photos of the Safi boulder field (photo courtesy of Barbara Theilen-Willige)

5 **4.3.5. Safi coast**

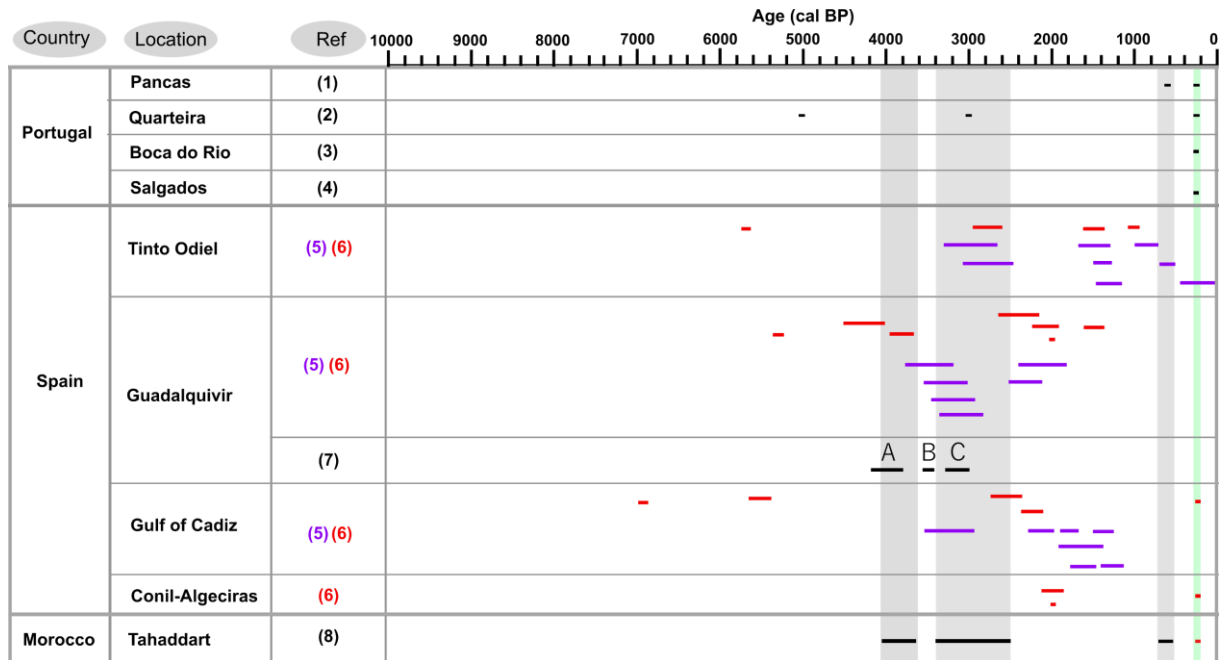
6 About 12 km south of Safi, Theilen-Willige et al. (2013) reported the presence of a few  
 7 boulders, located on the intertidal platform, either arranged in the form of an arc curved towards

1 the ocean or leaning directly on the cliffs present in this area (19 in Fig. 6b; Figs. 8d and 8e).  
2 Other blocks have been observed in overturned or upright positions with streak marks on the  
3 surface as evidence of their displacement by the waves. According to these authors, the weight  
4 of some blocks exceeds 100 tons.

## 5 **5. Chronological correlation of identified events with regional marine** 6 **submersion deposits**

7 To recognize possible regional events, the Moroccan marine submersion deposits have been  
8 chronologically correlated with other deposits along the Iberian coasts. The only deposits dated  
9 along the Moroccan Atlantic coast are those of Khalfaoui et al. (2020) and Khalfaoui (2021)  
10 (Fig. 9). The 1755 CE tsunami is the only confirmed event through both historical and  
11 geological approaches (Kaabouben et al. 2009; Khalfaoui et al. 2020). It is a well-documented  
12 regional tsunami with multiple deposits already identified and well-dated along the Spanish and  
13 Portuguese coasts, notably in the Salgado Lagoon (Costa et al. 2012), Boca Do Rio (Hindson  
14 and Andrade 1999), Martinhal (Kortekaas and Dawson 2007) and in the Gulf of Cadiz (Cuven  
15 et al. 2013). The three additional deposits dated by Khalfaoui (2021) around 3800, 2700 and  
16 625 cal BP are considered by the author as possible events. Further studies are needed to  
17 confirm their occurrence. However, they can also be correlated with some Spanish marine  
18 submersion deposits. For example, Rodríguez-Ramírez et al. (2015) recognised three marine  
19 submersion deposits from sedimentary records collected in the Guadalquivir estuary. The first  
20 one (event A) was dated around 4000 cal BP and was considered the most intense and  
21 destructive of the three events. According to the authors, it significantly transformed the  
22 geomorphology of the Guadalquivir estuary and impacted a human settlement in the region  
23 established during the Neolithic and Copper Age periods. Event B, dated at ~3550 cal BP, was  
24 considered of lesser magnitude compared to A. It was correlated with a 3600 cal BP earthquake,  
25 located through turbidite deposits identified by Vizcaino et al. (2006) on marine cores from the  
26 southwestern margin of Portugal. The third deposit (C) covered an extensive geographic area  
27 in the Doñana estuary and was dated at ~3150 cal BP. Taking into account the uncertainties of  
28 <sup>14</sup>C dating, it is possible to correlate between the 2700 and 3800 cal BP events in the Tahaddart  
29 estuary, respectively with the deposits A and C of Rodríguez-Ramírez et al. (2015). Other works  
30 on the Iberian Atlantic coasts agree on the existence of a submergence event between 3000 and  
31 2500 cal BP, whose sedimentary traces are present in Guardiana, Rio Piedras, Tinto-Odiel and  
32 Guadalquivir (see the review of Costa et al. 2022). Marine submersion deposit similar in term

1 of age to the 625 cal BP deposit was recognized by Morales et al. (2008) in the Tinto-Odeil  
 2 estuary, in the form of a marine shell-rich tsunamigenic level (HEL2). Another suspected  
 3 tsunami deposit was identified by Becker-Heidmann et al. (2007) near Cape Camarinal  
 4 (Bolonia), dated around 500 cal BP.



5  
 6 **Fig. 9** Chronological correlation between marine submersion deposits along the Spanish, Portuguese and Moroccan Atlantic coasts: (1)  
 7 (Andrade et al. 2003) ; (2) (Schneider et al. 2010) ; (3) (Dawson et al. 1995) ; (4) (Costa et al. 2012) ; (5) Compilation of tsunamigenic deposits  
 8 from Ruiz et al. 2013); (6) Compilation of tsunamigenic deposits from Lario et al. (2011b) ; (7) (Rodríguez-Ramírez et al. 2015b); (8)  
 9 (Khalfaoui 2021). A, B and C correspond to the events identified by Rodríguez-Ramírez et al., 2015b. The grey and green vertical bars  
 10 respectively correspond to possible and confirmed events

11 The three events detected by Raji et al. (2015) in the Nador lagoon are the only known and  
 12 dated marine submersion events along the Moroccan Mediterranean coast (the two tsunamis of  
 13 1522 and 1790 CE, and the storm surge of 1889 CE). The 1522 CE event has been recorded in  
 14 multiple sites along the Spanish coasts. Becker-Heidmann et al. (2007) managed to date this  
 15 event in Algeciras, using radiocarbon techniques (Fig. 10). Sedimentary evidences of the same  
 16 event were discovered by Reicherter and Becker-Heidmann (2009) in shallow drilling in the  
 17 lagoon of the Cabo de Gata area. According to historical records, the 1522 Almeria earthquake  
 18 affected large areas in the western Mediterranean and caused more than 1000 casualties  
 19 (Reicherter and Becker-Heidmann 2009).

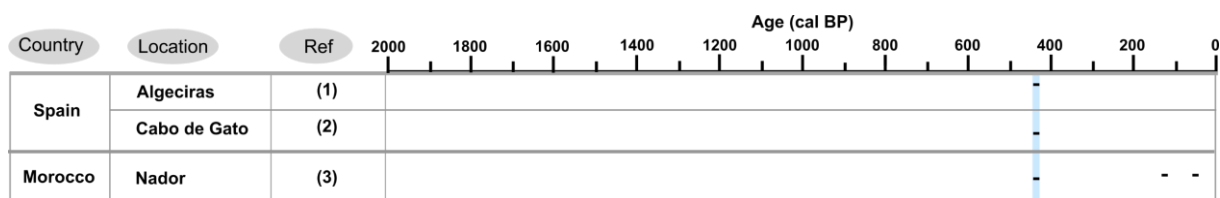


**Fig. 10** Chronological correlation between marine submersion deposits along the Spanish and Moroccan Mediterranean coasts: (1) (Becker-Heidmann et al. 2007); (2) (Reicherter and Becker-Heidmann 2009); (3) (Raji et al. 2015). The vertical green bar indicates confirmed events

## 6. Gaps and needs

The work done so far on the Moroccan coasts to document marine submersion deposits detected several coastal sites containing sedimentological evidence of these events. Despite this effort, the number of studies is very low compared to neighbouring countries (Spain and Portugal). Also, most of the detected sites are located along the Atlantic coast, which leave the Mediterranean side poorly studied. On the one hand, it is important to revisit all the investigated sites, to conduct more complete studies, especially on sediment cores that can cover a large period of time. On the other hand, several coastal sites have not yet been investigated and deserve to be prospected. On the Mediterranean coast, the lagoon of Smir seems to be a good spot to search for marine submersion deposits. The coastal dune separating the lagoon from the sea is not very high (2-4 m), and potentially submersible in the case of a tsunami or storm surge. On the Atlantic coasts, we can site the lagoons of Moulay Bouselham and Khenifiss, as well as the coastal lac of Sidi Boughaba.

The offshore part of the Moroccan coasts can be a valuable source of information on marine submersion events. Shallow sea and deep-sea canyon environments are also capable of retaining marine submersion deposits, especially tsunamis. A comprehensive compilation of studies concerning backwash deposits in marine shallow waters is given by Riou (2019). Beyond the storm-wave base, the high sedimentation rates can give rapid coverage for tsunami backwash deposits (Costa and Andrade 2020). Using sediment cores collected from the Pago Pago Bay (American Samoa), Riou et al. (2020) identified backwash deposits belonging to the 2009 south Pacific tsunami and the 1960 great Chilean earthquake tsunamis. The tsunami layers exhibited a sharp basal contact and were non- or poorly graded, compared to the background sedimentation. They also showed high values of Ti/Ca ratio, as a result of the land-sea transport of sediment (Riou et al. 2020). In the same sequences, the authors also recognized fine-grained terrestrial flashflood deposits belonging to tropical cyclones Ofa (1990 CE) or Val (1991 CE) and potential coarse-grained terrigenous run-off deposits emplaced during Cyclone Rene just four months after the 2009 SPT, or by Cyclone Wilma in early 2011. Quintela et al. (2016)



1 detected deposits belonging to the 1755 Lisbon tsunami on offshore records collected south of  
2 Portugal. The tsunami deposits were in the form of coarse layers, rich in coastal foraminifera  
3 species, compared to the background sedimentation (Quintela et al. 2016). It is worth  
4 mentioning that such an approach is challenging in offshore environments. The seafloor  
5 investigations and access to sediments are logistically difficult, expensive, and time-consuming  
6 (Schwarzer 2020). To find the right spot for sampling, a good knowledge of seafloor  
7 architecture, geomorphology, and sediment-distribution patterns is required.

8 The majority of marine submersion deposits identified along the Moroccan coasts lack  
9 chronological data, making it difficult to place them in a chronological framework.  
10 Consequently, the chronological correlation between marine submersion deposits located on  
11 the same site, or in different locations (e.g., regional scale), also becomes challenging. Without  
12 chronological data, there is no recurrence interval for these extreme events. For the few  
13 available  $^{14}\text{C}$  dates, the absence of a local DeltaR value poses another problem that needs to be  
14 dealt with. This value is usually used to calibrate  $^{14}\text{C}$  dates obtained on marine organisms. It  
15 represents the regional deviation from the pre-industrial marine reservoir age, estimated to be  
16  $\sim 400$   $^{14}\text{C}$  yr in subtropical oceans (Heaton et al. 2020). This local deviation from the marine  
17 reservoir age is caused by several factors such as upwelling currents, which are very abundant  
18 along the Atlantic coast of Morocco. Usually, the DeltaR value can be estimated by comparing  
19  $^{14}\text{C}$  dates obtained on pairs of contemporary marine and continental organisms, collected for  
20 example at the same depth in the same sediment core (or trench), or found at the same coastal  
21 archaeological site. In the Tahaddart estuary (NW of Morocco), Khalfaoui et al. (2020) tried to  
22 estimate this value using a pair of contemporary wood and marine shell, collected from the  
23 same depth in one of the studied cores. The authors found a value of  $-75 \pm 20$  years, which is  
24 relatively close to the one obtained by Martins and Soares (2013) for the Andalusian coast in  
25 Spain ( $-108 \pm 31$  years). However, the value obtained by Khalfaoui et al. (2020) must be taken  
26 with caution, since the oceanographic conditions are different between the different parts of the  
27 Moroccan Atlantic coast. Along the Mediterranean coast, Raji et al. (2015) found a DeltaR  
28 value of about  $-218$  years using sediment cores collected from the Nador lagoon. Additional  
29 studies are certainly needed to determine the geographical and temporal variation of DeltaR  
30 along the Moroccan coasts, which will help to precise the chronology of marine submersion  
31 deposits.

32 There is a great need to work in partnership with local historians and archaeologists to better  
33 understand the impact of these extreme events on the local population, which has occupied the

1 Moroccan coasts since the Neolithic phase. During the Roman period, trade activities, based on  
2 fishing, salt and garum production were probably affected by these disasters. For example, a  
3 sudden interruption of garum production in the 3rd century CE has been reported in several  
4 coastal archaeological sites in Spain, Portugal and Morocco. The origin is uncertain and may  
5 be political (fall of the Roman Empire) or natural, related to one or more extreme marine events  
6 (Alonso et al. 2015; Trakadas 2015; González-Regalado et al. 2018).

## 7 **7. Conclusion**

8 Marine submersion events represent a major threat to the Moroccan coastlines, especially with  
9 the current socio-economic development along the coasts and the future rise of the mean sea  
10 level caused by global warming. The study of coastal marine submersion deposits can help  
11 extend further back in time the Moroccan tsunami and storm surge records, to determine their  
12 return periods and maximum intensities. The first part of this work was a general overview of  
13 different types of geological signatures left by marine submersion events along the shores, such  
14 as boulders and washover deposits. The second part was a synthesis of the processes responsible  
15 for storm surges and tsunamis on the Moroccan coasts, as well as the sedimentary records  
16 produced by these events on these coasts. Storm surges on the Atlantic side are caused by  
17 extratropical cyclones, which circulate between the Azores High and the Icelandic Low mostly  
18 during the winter season. The Mediterranean coast is exposed to extratropical cyclones and  
19 sometimes to Medicans (Mediterranean cyclones). Tsunamis on the Atlantic coast are caused  
20 mainly by submarine earthquakes, generated by the Azores-Gibraltar seismic zone. On the  
21 Mediterranean side, tsunamis are less intense and are related mostly to the seismic activity of  
22 the strike-slip fault systems of the Alboran Sea. Several coastal sites revealed the presence of  
23 deposits belonging to these marine extreme events in the form of fine sediments and boulders.  
24 They are for the most part located on the Atlantic coast, especially along the Rabat-Bouznika  
25 coast and the Tahaddart-Cap Spartel coast.

26 Amid the gaps raised during this review is the still low number of studies on this topic in  
27 Morocco, compared to neighbouring countries (Spain and Portugal), and the lack of  
28 chronological data for most of the marine submersion deposits identified so far. Among the  
29 recommendations, it is important to revisit the already known sites and to conduct more  
30 complete studies using multiproxy approaches on sediment cores, which are capable of  
31 covering a larger time scale. In addition to the Moroccan continental shelf, some coastal sites

1 remain uninvestigated and deserve to be prospected, such as the Smir lagoon and the coastal  
2 lake of Sidi Boughaba.

### 3 **Acknowledgement**

4 This study was funded by MISTRALS/PALEOMEX, SICMED and Partenariat Hubert Curien  
5 (PHC) Toubkal (No. TBK/17/40 - Campus No. 36864YB; coordinated by Laurent Dezileau and  
6 Maria Snoussi).

### 7 **Competing interests**

8 The authors declare that they have no conflict of interest.

### 9 **References**

- 10 Abad M, Izquierdo T, Cáceres M, et al (2020) Coastal boulder deposit as evidence of an ocean-  
11 wide prehistoric tsunami originated on the Atacama Desert coast (northern Chile).  
12 *Sedimentology* 67:1505–1528
- 13 Abadie S, Paris A, Ata R, et al (2020) La Palma landslide tsunami: calibrated wave source and  
14 assessment of impact on French territories. *Natural Hazards and Earth System Sciences*  
15 20:3019–3038. <https://doi.org/10.5194/nhess-20-3019-2020>
- 16 Abadie SM, Harris JC, Grilli ST, Fabre R (2012) Numerical modeling of tsunami waves  
17 generated by the flank collapse of the Cumbre Vieja Volcano (La Palma, Canary  
18 Islands): Tsunami source and near field effects. *Journal of Geophysical Research:*  
19 *Oceans* 117:1–26. <https://doi.org/10.1029/2011JC007646>
- 20 Alfred R. Loeblich J, Tappaan H (1988) Foraminiferal genera and their classification
- 21 Alonso B, Ercilla G, García M, et al (2014) Quaternary mass-transport deposits on the north-  
22 eastern Alboran seamounts (SW Mediterranean Sea). In: *Submarine Mass Movements*  
23 *and Their Consequences*. Springer, pp 561–570
- 24 Alonso C, Gracia FJ, Rodríguez-Polo S, Martín Puertas C (2015) El registro de eventos  
25 energéticos marinos en la bahía de cádiz durante épocas históricas. *Cuaternario y*  
26 *Geomorfología* 29:95–117. <https://doi.org/10.17735/cyg.v29i1-2.29935>
- 27 Álvarez-Gómez JA, Aniel-Quiroga Í, González M, et al (2011) Scenarios for earthquake-  
28 generated tsunamis on a complex tectonic area of diffuse deformation and low velocity:  
29 The Alboran Sea, Western Mediterranean. *Marine Geology* 284:55–73.  
30 <https://doi.org/10.1016/j.margeo.2011.03.008>
- 31 Andrade C, Freitas MC, Miranda JM, et al (2003) Recognizing possible tsunami sediments in  
32 the ultradissipative environment of the Tagus estuary (Portugal)

- 1 Bahlburg H, Weiss R (2007) Sedimentology of the December 26, 2004, Sumatra tsunami  
2 deposits in eastern India (Tamil Nadu) and Kenya. *International Journal of Earth*  
3 *Sciences* 96:1195–1209. <https://doi.org/10.1007/s00531-006-0148-9>
- 4 Ballarini M, Wallinga J, Murray AS, et al (2003) Optical dating of young coastal dunes on a  
5 decadal time scale. *Quaternary Science Reviews* 22:1011–1017.  
6 [https://doi.org/10.1016/S0277-3791\(03\)00043-X](https://doi.org/10.1016/S0277-3791(03)00043-X)
- 7 Baptista MA, Heitor S, Miranda JM, et al (1998) The 1755 Lisbon tsunami; evaluation of the  
8 tsunami parameters. *Journal of Geodynamics* 25:143–157.  
9 [https://doi.org/10.1016/S0264-3707\(97\)00019-7](https://doi.org/10.1016/S0264-3707(97)00019-7)
- 10 Baptista MA, Miranda JM (2009) Revision of the portuguese catalog of tsunamis. *Natural*  
11 *Hazards and Earth System Science* 9:25–42. <https://doi.org/10.5194/nhess-9-25-2009>
- 12 Baumann J, Chaumillon E, Schneider JL, et al (2017) Contrasting sediment records of marine  
13 submersion events related to wave exposure, Southwest France. *Sedimentary Geology*  
14 353:158–170. <https://doi.org/10.1016/j.sedgeo.2017.03.009>
- 15 Becker-Heidmann P, Reicherter K, Silva PG (2007) 14C-Dated Charcoal and Sediment Drilling  
16 Cores as First Evidence of Holocene Tsunamis at the Southern Spanish Coast.  
17 *Radiocarbon* 49:827–835. <https://doi.org/10.1017/S0033822200042703>
- 18 Belkhat Z, Aoula RE, Mhammdi N (2017) Effects of the winter storms of 2017 on the  
19 Atlantic coast of Rabat: A preliminary evaluation Effets des tempêtes hivernales de  
20 2017 sur la côte Atlantique de Rabat : Evaluation préliminaire. 135–139
- 21 Biester H, Keppler F, Putschew A, et al (2004) Halogen Retention, Organohalogenes, and the  
22 Role of Organic Matter Decomposition on Halogen Enrichment in Two Chilean Peat  
23 Bogs. *Environmental Science & Technology* 38:1984–1991.  
24 <https://doi.org/10.1021/es0348492>
- 25 Biguenet M, Sabatier P, Chaumillon E, et al (2021) A 1600 year-long sedimentary record of  
26 tsunamis and hurricanes in the Lesser Antilles (Scrub Island, Anguilla). *Sedimentary*  
27 *Geology* 412:105806. <https://doi.org/10.1016/j.sedgeo.2020.105806>
- 28 Brill D, May SM, Mhammdi N, et al (2021) Evaluating optically stimulated luminescence rock  
29 surface exposure dating as a novel approach for reconstructing coastal boulder  
30 movement on decadal to centennial timescales. *Earth Surf Dynam* 9:205–234.  
31 <https://doi.org/10.5194/esurf-9-205-2021>
- 32 Brill D, Tamura T (2020) Optically stimulated luminescence dating of tsunami and storm  
33 deposits. In: *Geological Records of Tsunamis and Other Extreme Waves*. Elsevier, pp  
34 705–727
- 35 Campos ML (1991) Tsunami hazard on the Spanish coasts of the Iberian Peninsula. *Science of*  
36 *Tsunami Hazards* 9:83–90
- 37 Carmona P, Ruiz JM (2009) Geomorphological evolution of the River Loukkos estuary around  
38 the Phoenician City of Lixus on the Atlantic Littoral of Morocco. *Geoarchaeology*  
39 24:821–845. <https://doi.org/10.1002/gea.20289>

- 1 Casas D, Ercilla G, Yenes M, et al (2011) The Baraza Slide: model and dynamics. *Mar Geophys*  
2 *Res* 32:245–256. <https://doi.org/10.1007/s11001-011-9132-2>
- 3 Chagué C (2020) Applications of geochemical proxies in paleotsunami research. In: *Geological*  
4 *Records of Tsunamis and Other Extreme Waves*. pp 381–401
- 5 Chagué-Goff C (2010) Chemical signatures of palaeotsunamis: A forgotten proxy? *Marine*  
6 *Geology* 271:67–71. <https://doi.org/10.1016/j.margeo.2010.01.010>
- 7 Chagué-Goff C, Andrew A, Szczuciński W, et al (2012) Geochemical signatures up to the  
8 maximum inundation of the 2011 Tohoku-oki tsunami — Implications for the 869AD  
9 Jogan and other palaeotsunamis. *Sedimentary Geology* 282:65–77.  
10 <https://doi.org/10.1016/j.sedgeo.2012.05.021>
- 11 Chagué-Goff C, Fyfe WS (1996) Geochemical and petrographical characteristics of a domed  
12 bog, Nova Scotia: a modern analogue for temperate coal deposits. *Organic*  
13 *Geochemistry* 24:141–158. [https://doi.org/10.1016/0146-6380\(96\)00014-9](https://doi.org/10.1016/0146-6380(96)00014-9)
- 14 Chagué-Goff C, Schneider JL, Goff JR, et al (2011) Expanding the proxy toolkit to help identify  
15 past events - Lessons from the 2004 Indian Ocean Tsunami and the 2009 South Pacific  
16 Tsunami. *Earth-Science Reviews* 107:107–122.  
17 <https://doi.org/10.1016/j.earscirev.2011.03.007>
- 18 Chagué-Goff C, Szczuciński W, Shinozaki T (2017) Applications of geochemistry in tsunami  
19 research: A review. *Earth-Science Reviews* 165:203–244.  
20 <https://doi.org/10.1016/j.earscirev.2016.12.003>
- 21 Chahid D, Lenoble A, Boudad L, Vliet-Lanoë BV (2016) Enregistrements sédimentaires  
22 d'événements de haute énergie, exemples de la côte atlantique de Rabat-Skhirat  
23 (Maroc). *Quaternaire* 155–169. <https://doi.org/10.4000/quaternaire.7543>
- 24 Chiguer A, Medina F (2019) Emplacement of high-energy mega-boulders along the atlantic  
25 coast of Rabat (Morocco). *Geogaceta* 66:15–18
- 26 Choowong M, Murakoshi N, Hisada K, et al (2008) Flow conditions of the 2004 Indian Ocean  
27 tsunami in Thailand, inferred from capping bedforms and sedimentary structures. *Terra*  
28 *Nova* 20:141–149. <https://doi.org/10.1111/j.1365-3121.2008.00799.x>
- 29 Costa PJM, Andrade C (2020) Tsunami deposits: Present knowledge and future challenges.  
30 *Sedimentology* 67:1189–1206. <https://doi.org/10.1111/sed.12724>
- 31 Costa PJM, Andrade C, Freitas MC, et al (2011) Boulder deposition during major tsunami  
32 events. *Earth Surface Processes and Landforms* 36:2054–2068.  
33 <https://doi.org/10.1002/esp.2228>
- 34 Costa PJM, Andrade C, Freitas MC, et al (2012) A tsunami record in the sedimentary archive  
35 of the central Algarve coast, Portugal: Characterizing sediment, reconstructing sources  
36 and inundation paths. *The Holocene* 22:899–914.  
37 <https://doi.org/10.1177/0959683611434227>

- 1 Costa PJM, Dawson S, Ramalho RS, et al (2021) A review on onshore tsunami deposits along  
2 the Atlantic coasts. *Earth-Science Reviews* 212:103441.  
3 <https://doi.org/10.1016/j.earscirev.2020.103441>
- 4 Costa PJM, Lario J, Reicherter K (2022) Tsunami Deposits in Atlantic Iberia: A Succinct  
5 Review. In: Álvarez-Martí-Aguilar M, Machuca Prieto F (eds) *Historical Earthquakes,*  
6 *Tsunamis and Archaeology in the Iberian Peninsula.* Springer Nature, Singapore, pp  
7 105–126
- 8 Cox R, Arduin F, Dias F, et al (2020) Systematic Review Shows That Work Done by Storm  
9 Waves Can Be Misinterpreted as Tsunami-Related Because Commonly Used  
10 Hydrodynamic Equations Are Flawed. *Front Mar Sci* 7:4.  
11 <https://doi.org/10.3389/fmars.2020.00004>
- 12 Cox R, O'boyle L, Cytrynbaum J (2019) Imbricated coastal boulder deposits are formed by  
13 storm waves, and can preserve a long-term storminess record. *Scientific Reports* 9:1–  
14 12. <https://doi.org/10.1038/s41598-019-47254-w>
- 15 Croudace IW, Rothwell RG (2015) *Micro-XRF Studies of Sediment Cores. Applications of a*  
16 *Non-destructive Tool for the Environmental Sciences*
- 17 Cundy AB, Kortekaas S, Dewez T, et al (2000) Coastal wetlands as recorders of earthquake  
18 subsidence in the Aegean: a case study of the 1894 Gulf of Atalantiearthquakes, central  
19 Greece. *Marine Geology* 170:3–26. [https://doi.org/10.1016/S0025-3227\(00\)00062-1](https://doi.org/10.1016/S0025-3227(00)00062-1)
- 20 Cuven S, Paris R, Falvard S, et al (2013) High-resolution analysis of a tsunami deposit: Case-  
21 study from the 1755 Lisbon tsunami in southwestern Spain. *Marine Geology* 337:98–  
22 111. <https://doi.org/10.1016/j.margeo.2013.02.002>
- 23 Dawson AG (1994) Geomorphological effects of tsunami run-up and backwash.  
24 *Geomorphology* 10:83–94. [https://doi.org/10.1016/0169-555X\(94\)90009-4](https://doi.org/10.1016/0169-555X(94)90009-4)
- 25 Dawson AG (2000) Tsunami Deposits. *Pure and Applied Geophysics* 157:875–897.  
26 <https://doi.org/10.1007/s000240050010>
- 27 Dawson AG, Hindson R, Andrade C, et al (1995) Tsunami sedimentation associated with the  
28 Lisbon earthquake of 1 November AD 1755: Boca do Rio, Algarve, Portugal. *The*  
29 *Holocene* 5:209–215. <https://doi.org/10.1177/095968369500500208>
- 30 Degeai JP, Devillers B, Dezileau L, et al (2015) Major storm periods and climate forcing in the  
31 Western Mediterranean during the Late Holocene. *Quaternary Science Reviews*  
32 129:37–56. <https://doi.org/10.1016/j.quascirev.2015.10.009>
- 33 Dezileau L, Pérez-Ruzafa A, Blanchemanche P, et al (2016) Extreme storms during the last  
34 6500 years from lagoonal sedimentary archives in the Mar Menor (SE Spain). *Climate*  
35 *of the Past* 12:1389–1400. <https://doi.org/10.5194/cp-12-1389-2016>
- 36 Dezileau L, Sabatier P, Blanchemanche P, et al (2011) Intense storm activity during the Little  
37 Ice Age on the French Mediterranean coast. *Palaeogeography, Palaeoclimatology,*  
38 *Palaeoecology* 299:289–297. <https://doi.org/10.1016/j.palaeo.2010.11.009>

- 1 Donnelly J, Goff J, Chagué-Goff C (2017) A record of local storms and trans-Pacific tsunamis,  
2 eastern Banks Peninsula, New Zealand. *Holocene* 27:496–508.  
3 <https://doi.org/10.1177/0959683616670222>
- 4 Dutta K (2008) Marine 14C reservoir age and Suess effect in the Indian Ocean. *Earth Sci India*  
5 1:243–257
- 6 El Messaoudi B, Ait Laâmel M, El Hou M, Bouksim H (2016) Situations des fortes houles sur  
7 les côtes atlantiques marocaines. *Actes Session Plénière Académie Hassan II des*  
8 *Sciences & Techniques* 79–99
- 9 El Talibi H (2016) Evidences of tsunami deposits along the Moroccan Atlantic coast (Tanger-  
10 Asilah): Methodological approach, sites analyses and hazard mitigation
- 11 El Talibi H, El Moussaoui S, Aboumaria K, et al (2020) Geological evidence of high-energy  
12 marine flooding events on the Tangier coastal plain, Morocco. *Euro-Mediterr J Environ*  
13 *Integr* 6:7. <https://doi.org/10.1007/s41207-020-00215-6>
- 14 El Talibi H, El Moussaoui S, Zaghoul MN, et al (2016) New sedimentary and geomorphic  
15 evidence of tsunami flooding related to an older events along the Tangier-Asilah coastal  
16 plain, Morocco. *Geoenvironmental Disasters* 3:14–14. [https://doi.org/10.1186/s40677-](https://doi.org/10.1186/s40677-016-0049-6)  
17 [016-0049-6](https://doi.org/10.1186/s40677-016-0049-6)
- 18 Engel M, Pilarczyk J, May SM, et al (2020) *Geological Records of Tsunamis and Other*  
19 *Extreme Waves*. Elsevier
- 20 Fine IV, Rabinovich AB, Bornhold BD, et al (2005) The Grand Banks landslide-generated  
21 tsunami of November 18, 1929: preliminary analysis and numerical modeling. *Marine*  
22 *Geology* 215:45–57
- 23 Finkl CW, Makowski C (eds) (2019) *Encyclopedia of Coastal Science*. Springer International  
24 Publishing, Cham
- 25 García-Mayordomo J, Insua-Arévalo JM, Martínez-Díaz JJ, et al (2012) The Quaternary Active  
26 Faults Database of Iberia (QAFI v.2.0). *Journal of Iberian Geology* 38:285–302.  
27 [https://doi.org/10.5209/rev\\_JIGE.2012.v38.n1.39219](https://doi.org/10.5209/rev_JIGE.2012.v38.n1.39219)
- 28 Genet P-E (2011) Signature sédimentaire des tsunamis sur la côte atlantique marocaine entre  
29 Tanger et Larache et implications en terme de risque
- 30 Gigout M (1959) Ages par radiocarbone de deux formations des environs de Rabat (Maroc).  
31 *Comptes rendu hebdomadaires des seances de l'acadimie des sciences* 249:2802–2803
- 32 Gigout M (1957) L'Ouljien dans le cadre du Tyrrhenien. *Bulletin de la Société Géologique de*  
33 *France* S6-VII:385–400. <https://doi.org/10.2113/gssgfbull.S6-VII.4-5.385>
- 34 Goff J, Chagué-Goff C, Nichol S (2001) Palaeotsunami deposits: a New Zealand perspective.  
35 *Sedimentary Geology* 143:1–6. [https://doi.org/10.1016/S0037-0738\(01\)00121-X](https://doi.org/10.1016/S0037-0738(01)00121-X)
- 36 González-Regalado ML, Gómez P, Ruiz F, et al (2018) Holocene palaeoenvironmental  
37 evolution of Saltés Island (Tinto and Odiel estuary, SW Spain) during the Roman period

- 1 (1st century BC–5th century AD). *Journal of Iberian Geology*.  
2 <https://doi.org/10.1007/s41513-018-0089-8>
- 3 Goto K, Kawana T, Imamura F (2010) Historical and geological evidence of boulders deposited  
4 by tsunamis, southern Ryukyu Islands, Japan. *Earth-Science Reviews* 102:77–99.  
5 <https://doi.org/10.1016/j.earscirev.2010.06.005>
- 6 Goto K, Miyagi K, Kawana T, et al (2011) Emplacement and movement of boulders by known  
7 storm waves — Field evidence from the Okinawa Islands, Japan. *Marine Geology*  
8 283:66–78. <https://doi.org/10.1016/j.margeo.2010.09.007>
- 9 Gràcia E, Dañobeitia J, Vergés J, Team P (2003) Mapping active faults offshore Portugal  
10 (36°N–38°N): Implications for seismic hazard assessment along the southwest Iberian  
11 margin. *Geology* 31:83–86. [https://doi.org/10.1130/0091-  
12 7613\(2003\)031<0083:MAFOPN>2.0.CO;2](https://doi.org/10.1130/0091-7613(2003)031<0083:MAFOPN>2.0.CO;2)
- 13 Guilbault J-P, Clague JJ, Lapointe M (1996) Foraminiferal evidence for the amount of  
14 coseismic subsidence during a late holocene earthquake on Vancouver Island, West  
15 Coast of Canada. *Quaternary Science Reviews* 15:913–937.  
16 [https://doi.org/10.1016/S0277-3791\(96\)00058-3](https://doi.org/10.1016/S0277-3791(96)00058-3)
- 17 Gutscher M-A (2006) The great Lisbon earthquake and tsunami of 1755: lessons from the recent  
18 Sumatra earthquakes and possible link to Plato's Atlantis. *European Review* 14:181–  
19 191. <https://doi.org/10.1017/S1062798706000184>
- 20 Hall AM, Hansom JD, Williams DM (2010) Wave-emplaced coarse debris and megaclasts in  
21 Ireland and Scotland: boulder transport in a high-energy littoral environment: a  
22 discussion. *The Journal of Geology* 118:699–704
- 23 Hall AM, Hansom JD, Williams DM, Jarvis J (2006) Distribution, geomorphology and  
24 lithofacies of cliff-top storm deposits: Examples from the high-energy coasts of  
25 Scotland and Ireland. *Marine Geology* 232:131–155.  
26 <https://doi.org/10.1016/j.margeo.2006.06.008>
- 27 Hallegatte S, Green C, Nicholls RJ, Corfee-Morlot J (2013) Future flood losses in major coastal  
28 cities. *Nature climate change* 3:802–806
- 29 Haut Commissariat au Plan (2014) Répartition géographique de la population d'après les  
30 données du recensement général de la population et de l'habitat de 2014. Rapport Final  
31 Direction de la statistique
- 32 Hawkes AD, Bird M, Cowie S, et al (2007) Sediments deposited by the 2004 Indian Ocean  
33 Tsunami along the Malaysia–Thailand Peninsula. *Marine Geology* 242:169–190.  
34 <https://doi.org/10.1016/j.margeo.2007.02.017>
- 35 Hayward BW, Grenfell HR, Reid CM, Hayward KA (1999) Recent New Zealand shallow-water  
36 benthic foraminifera: Taxonomy, ecologic distribution, biogeography, and use in  
37 paleoenvironmental assessment. *Institute of Geological and Nuclear Sciences*  
38 *Monograph* 21:264–264



- 1 Heaton TJ, Köhler P, Butzin M, et al (2020) Marine20—The Marine Radiocarbon Age  
2 Calibration Curve (0–55,000 cal BP). *Radiocarbon* 62:779–820.  
3 <https://doi.org/10.1017/RDC.2020.68>
- 4 Hindson RA, Andrade C (1999) Sedimentation and hydrodynamic processes associated with  
5 the tsunami generated by the 1755 Lisbon earthquake. *Quaternary International* 56:27–  
6 38. [https://doi.org/10.1016/S1040-6182\(98\)00014-7](https://doi.org/10.1016/S1040-6182(98)00014-7)
- 7 Hindson RA, Andrade C, Dawson AG (1996) Sedimentary processes associated with the  
8 tsunami generated by the 1755 Lisbon earthquake on the Algarve coast, Portugal.  
9 *Physics and Chemistry of the Earth* 21:57–63. [https://doi.org/10.1016/S0079-  
10 1946\(97\)00010-4](https://doi.org/10.1016/S0079-1946(97)00010-4)
- 11 Jaffe BE, Morton RA, Kortekaas S, et al (2008) Reply to Bridge (2008) Discussion of articles  
12 in “Sedimentary features of tsunami deposits.” *Sedimentary Geology* 211:95–97.  
13 <https://doi.org/10.1016/j.sedgeo.2008.08.006>
- 14 Johnston AC (1996) Seismic moment assessment of earthquakes in stable continental regions—  
15 III. New Madrid 1811–1812, Charleston 1886 and Lisbon 1755. *Geophysical Journal  
16 International* 126:314–344. <https://doi.org/10.1111/j.1365-246X.1996.tb05294.x>
- 17 Kaabouben F, Baptista MA, Iben Brahim A, et al (2009) On the moroccan tsunami catalogue.  
18 *Natural Hazards and Earth System Sciences* 9:1227–1236.  
19 <https://doi.org/10.5194/nhess-9-1227-2009>
- 20 Kelsey HM, Witter RC (2020) Radiocarbon dating of tsunami and storm deposits. In:  
21 *Geological Records of Tsunamis and Other Extreme Waves*. Elsevier, pp 663–685
- 22 Khalifaoui O (2021) Reconstitution des paléo-submersions marines (tsunamis et tempêtes) le  
23 long de la côte Atlantique Nord du Maroc au cours des derniers millénaires. These de  
24 doctorat, Normandie
- 25 Khalifaoui O, Dezileau L, Degeai JP, Snoussi M (2020) A late Holocene record of marine high-  
26 energy events along the Atlantic coast of Morocco: new evidences from the Tahaddart  
27 estuary. *Geoenvironmental Disasters* 7:. <https://doi.org/10.1186/s40677-020-00169-5>
- 28 Kortekaas S, Dawson AG (2007) Distinguishing tsunami and storm deposits: An example from  
29 Martinhal, SW Portugal. *Sedimentary Geology* 200:208–221.  
30 <https://doi.org/10.1016/j.sedgeo.2007.01.004>
- 31 Kozak JT, Moreira VS, Oldroyd DR (2005) Iconography of the 1755 Lisbon earthquake.  
32 *Geophysical Institute of the Academy of Sciences of the Czech Republic*
- 33 Lario J, Zazo C, Goy JL, et al (2011) Holocene palaeotsunami catalogue of SW Iberia.  
34 *Quaternary International* 242:196–200. <https://doi.org/10.1016/j.quaint.2011.01.036>
- 35 Leorri E, Freitas MC, Zourarah B, et al (2010) Multiproxy approach to characterize an  
36 overwash deposit: Oualidia lagoon (Moroccan Atlantic coast). *Geogaceta* 7–10
- 37 Li L, Switzer AD, Wang Y, et al (2018) A modest 0.5-m rise in sea level will double the tsunami  
38 hazard in Macau. *Science Advances* 4:1–12. <https://doi.org/10.1126/sciadv.aat1180>

- 1 Lopes V, Freitas MC, Zourarah B, et al (2010) Caracterização de depósito de galgamento no  
2 ambiente de barreira da laguna de Oualidia ( costa Atlântica Marroquina ). Revista  
3 Electrónica de Ciências da Terra X:2–5
- 4 Luque L, Lario J, Civis J, et al (2002) Sedimentary record of a tsunami during Roman times,  
5 Bay of Cadiz, Spain. Journal of Quaternary Science 17:623–631.  
6 <https://doi.org/10.1002/jqs.711>
- 7 Macías J, Vázquez JT, Fernández-Salas LM, et al (2015) The Al-Borani submarine landslide  
8 and associated tsunami. A modelling approach. Marine Geology 361:79–95.  
9 <https://doi.org/10.1016/j.margeo.2014.12.006>
- 10 Mamo B, Strotz L, Dominey-howes D (2009) Earth-Science Reviews Tsunami sediments and  
11 their foraminiferal assemblages. Earth Science Reviews 96:263–278.  
12 <https://doi.org/10.1016/j.earscirev.2009.06.007>
- 13 Maouche S, Morhange C, Meghraoui M (2009) Large boulder accumulation on the Algerian  
14 coast evidence tsunami events in the western Mediterranean. Marine Geology 262:96–  
15 104
- 16 Maramai A, Brizuela B, Graziani L (2014) The euro-mediterranean Tsunami catalogue. Annals  
17 of Geophysics 57:. <https://doi.org/10.4401/ag-6437>
- 18 Martins JMM, Soares AMM (2013) Marine Radiocarbon Reservoir Effect in Southern Atlantic  
19 Iberian Coast. Radiocarbon 55:1123–1134.  
20 <https://doi.org/10.1017/S0033822200048037>
- 21 Matias L, Ribeiro A, Baptista MA, et al (2005) Comment on “Lisbon 1755: A Case of Triggered  
22 Onshore Rupture?” by Susana P. Vilanova, Catarina F. Nunes, and Joao F. B. D.  
23 Fonseca. Bulletin of the Seismological Society of America 95:2534–2538.  
24 <https://doi.org/10.1785/0120040023>
- 25 Matthews JA (2012) The SAGE Handbook of Environmental Change: Volume 1: Approaches,  
26 Evidences and Causes Volume 2: Human Impacts and Responses. Sage
- 27 Medina F, Mhammdi N, Chiguer A, et al (2011) The Rabat and Larache boulder fields; new  
28 examples of high-energy deposits related to storms and tsunami waves in north-western  
29 Morocco. Natural Hazards 59:725–747. <https://doi.org/10.1007/s11069-011-9792-x>
- 30 Medina F, Mhammdi N, Emran A, Hakdaoui S (2018) A case of uplift and transport of a large  
31 boulder by the recent winter storms at Dahomey beach (Morocco). p 2
- 32 Mellas S (2012) Atlantique marocain Evaluation du risque tsunamique sur le littoral atlantique  
33 marocain
- 34 Mhammdi N, Medina F, Belkhat Z, et al (2020) Marine storms along the Moroccan Atlantic  
35 coast: An underrated natural hazard? Journal of African Earth Sciences 163:103730–  
36 103730. <https://doi.org/10.1016/j.jafrearsci.2019.103730>
- 37 Mhammdi N, Medina F, Kelletat D, et al (2008) Large boulders along the Rabat coast  
38 (Morocco); possible emplacement by the November, 1st, 1755 AD tsunami. Science of  
39 Tsunami Hazards 27:17–30

- 1 Mhammdi N, Medina F, Trentesaux A, et al (2015) Sedimentary Evidence of Palaeo-Tsunami  
2 Deposits Along the Loukkos Estuary (Moroccan Atlantic Coast). *Journal of Tsunami*  
3 *Society International* 32:77–95
- 4 Minoubi A, El khalidi K, Chaibi M, et al (2013) Variation morphosédimentaire saisonnière et  
5 impact de la tempête de Janvier 2009 sur la côte de Safi. *Maroc ScienceLib* 5:23–23
- 6 Minoura K, Nakaya S, Uchida M (1994) Tsunami deposits in a lacustrine sequence of the  
7 Sanriku coast, northeast Japan. *Sedimentary Geology* 89:25–31.  
8 [https://doi.org/10.1016/0037-0738\(94\)90081-7](https://doi.org/10.1016/0037-0738(94)90081-7)
- 9 Moore JG, Bryan WB, Ludwig KR (1994) Chaotic deposition by a giant wave, Molokai,  
10 Hawaii. *Geological Society of America Bulletin* 106:962–967.  
11 [https://doi.org/10.1130/0016-7606\(1994\)106<0962:CDBAGW>2.3.CO;2](https://doi.org/10.1130/0016-7606(1994)106<0962:CDBAGW>2.3.CO;2)
- 12 Morales JA, Borrego J, San Miguel EG, et al (2008) Sedimentary record of recent tsunamis in  
13 the Huelva Estuary (southwestern Spain). *Quaternary Science Reviews* 27:734–746.  
14 <https://doi.org/10.1016/j.quascirev.2007.12.002>
- 15 Morton RA, Gelfenbaum G, Jaffe BE (2007) Physical criteria for distinguishing sandy tsunami  
16 and storm deposits using modern examples. *Sedimentary Geology* 200:184–207.  
17 <https://doi.org/10.1016/j.sedgeo.2007.01.003>
- 18 Nagai R, Takabatake T, Esteban M, et al (2020) Tsunami risk hazard in Tokyo Bay: The  
19 challenge of future sea level rise. *International Journal of Disaster Risk Reduction*  
20 45:101321. <https://doi.org/10.1016/j.ijdr.2019.101321>
- 21 Nandasena NAK (2020) Chapter 29 - Perspective of incipient motion formulas: boulder  
22 transport by high-energy waves. In: Engel M, Pilarczyk J, May SM, et al. (eds)  
23 *Geological Records of Tsunamis and Other Extreme Waves*. Elsevier, pp 641–659
- 24 Niazi S (2007) Evaluation des impacts des changements climatiques et de l'élévation du niveau  
25 de la mer sur le littoral de Tétouan (méditerranée occidentale du Maroc): Vulnérabilité  
26 et Adaptation. Université Mohammed V
- 27 Nichols G (1999) *Sedimentology and Stratigraphy* Blackwell Publishing
- 28 Nichols G (2009) *Sedimentology and stratigraphy*. John Wiley & Sons
- 29 Noormets R, Felton EA, Crook KAW (2002) Sedimentology of rocky shorelines: 2: Shoreline  
30 megaclasts on the north shore of Oahu, Hawaii—origins and history. *Sedimentary*  
31 *Geology* 150:31–45
- 32 Ota Y, Shyu JBH, Wang C-C, et al (2015) Coral boulders along the coast of the Lanyu Island,  
33 offshore southeastern Taiwan, as potential paleotsunami records. *Journal of Asian Earth*  
34 *Sciences* 114:588–600. <https://doi.org/10.1016/j.jseaes.2015.08.001>
- 35 Pachauri RK, Allen MR, Barros VR, et al (2014) Climate change 2014: synthesis report.  
36 Contribution of Working Groups I, II and III to the fifth assessment report of the  
37 Intergovernmental Panel on Climate Change. Ipcc

- 1 Papadopoulos GA, Fokaefs A (2005) Strong tsunamis in the Mediterranean Sea: a re-  
2 evaluation. *ISSET Journal of Earthquake Technology* 42:159–170
- 3 Paris R, Fournier J, Poizot E, et al (2010) Boulder and fine sediment transport and deposition  
4 by the 2004 tsunami in Lhok Nga (western Banda Aceh, Sumatra, Indonesia): a coupled  
5 offshore–onshore model. *Marine Geology* 268:43–54
- 6 Paris R, Naylor LA, Stephenson WJ (2011) Boulders as a signature of storms on rock coasts.  
7 *Marine Geology* 283:1–11. <https://doi.org/10.1016/j.margeo.2011.03.016>
- 8 Phantuwongraj S, Choowong M, Nanayama F, et al (2013) Coastal geomorphic conditions and  
9 styles of storm surge washover deposits from Southern Thailand. *Geomorphology*  
10 192:43–58. <https://doi.org/10.1016/j.geomorph.2013.03.016>
- 11 Pilarczyk JE, Dura T, Horton BP, et al (2014) Microfossils from coastal environments as  
12 indicators of paleo-earthquakes, tsunamis and storms. *Palaeogeography,*  
13 *Palaeoclimatology,* *Palaeoecology* 413:144–157.  
14 <https://doi.org/10.1016/j.palaeo.2014.06.033>
- 15 Pörtner H-O, Roberts DC, Masson-Delmotte V, et al (2019) The ocean and cryosphere in a  
16 changing climate
- 17 Pouzet P, Maanan M (2020) Temporal approaches of historical extreme storm events based on  
18 sedimentological archives. *Journal of African Earth Sciences* 103710–103710.  
19 <https://doi.org/10.1016/j.jafrearsci.2019.103710>
- 20 Quintela M, Costa PJM, Fatela F, et al (2016) The AD 1755 tsunami deposits onshore and  
21 offshore of Algarve (south Portugal): sediment transport interpretations based on the  
22 study of Foraminifera assemblages. *Quaternary International* 408:123–138
- 23 Raji O (2014) Événements extrêmes du passé et paléoenvironnements : reconstitution à partir  
24 des archives sédimentaires de la lagune de Nador, Maroc. Université Mohammed V-  
25 Agdal, Faculté des Sciences, Rabat
- 26 Raji O, Dezileau L, Tessier B, et al (2018) Climate and tectonic-driven sedimentary infill of a  
27 lagoon as revealed by high resolution seismic and core data (the Nador lagoon, NE  
28 Morocco). *Marine Geology* 398:99–111. <https://doi.org/10.1016/j.margeo.2018.01.010>
- 29 Raji O, Dezileau L, Von Grafenstein U, et al (2015) Extreme sea events during the last  
30 millennium in the northeast of Morocco. *Natural Hazards and Earth System Sciences*  
31 15:203–211. <https://doi.org/10.5194/nhess-15-203-2015>
- 32 Ramalho RS, Winckler G, Madeira J, et al (2015) Hazard potential of volcanic flank collapses  
33 raised by new megatsunami evidence. *Science advances* 1:e1500456–e1500456
- 34 Regnaud H, Oszwald J, Planchon O, et al (2010) Polygenetic (tsunami and storm) deposits? A  
35 case study from Ushant Island, western France. *Zeitschrift für Geomorphologie,*  
36 *Supplementary Issues* 54:197–217
- 37 Reicherter K, Becker-Heidmann P (2009) Tsunami deposits in the western Mediterranean:  
38 remains of the 1522 Almería earthquake? Geological Society, London, Special  
39 Publications 316:217–235. <https://doi.org/10.1144/SP316.14>

- 1 Richmond BM, Buckley M, Etienne S, et al (2011) Deposits, flow characteristics, and landscape  
2 change resulting from the September 2009 South Pacific tsunami in the Samoan islands.  
3 *Earth-Science Reviews* 107:38–51
- 4 Riou B (2019) Shallow marine sediment record of tsunamis : analysis of the sediment-fill of the  
5 bays of Tutuila (American Samoa) and backwash deposits of the 2009 South Pacific  
6 Tsunami. These de doctorat, La Rochelle
- 7 Riou B, Chaumillon E, Chagué C, et al (2020) Backwash sediment record of the 2009 South  
8 Pacific Tsunami and 1960 Great Chilean Earthquake Tsunami. *Sci Rep* 10:4149.  
9 <https://doi.org/10.1038/s41598-020-60746-4>
- 10 Rodriguez M, Maleuvre C, Jollivet-Castelot M, et al (2017) Tsunamigenic submarine landslides  
11 along the Xauen–Tofiño banks in the Alboran Sea (Western Mediterranean Sea).  
12 *Geophysical Journal International* 209:266–281. <https://doi.org/10.1093/gji/ggx028>
- 13 Rodríguez-Ramírez A, Pérez-Asensio JN, Santos A, et al (2015a) Atlantic extreme wave events  
14 during the last four millennia in the Guadalquivir estuary, SW Spain. *Quaternary*  
15 *Research (United States)* 83:24–40. <https://doi.org/10.1016/j.yqres.2014.08.005>
- 16 Rodríguez-Ramírez A, Pérez-Asensio JN, Santos A, et al (2015b) Atlantic extreme wave events  
17 during the last four millennia in the Guadalquivir estuary, SW Spain. *Quaternary*  
18 *Research (United States)* 83:24–40. <https://doi.org/10.1016/j.yqres.2014.08.005>
- 19 Roger J, Baptista MA, Mosher D, et al (2010) Tsunami impact on Newfoundland, Canada, due  
20 to far-field generated tsunamis. Implications on hazard assessment. pp 2625–2630
- 21 Roger J, Hébert H, Ruegg J-C, Briole P (2011) The El Asnam 1980 October 10 inland  
22 earthquake: a new hypothesis of tsunami generation. *Geophysical Journal International*  
23 185:1135–1146. <https://doi.org/10.1111/j.1365-246X.2011.05003.x>
- 24 Ruiz F, Rodríguez-Vidal J, Abad M, et al (2013) Sedimentological and geomorphological  
25 imprints of Holocene tsunamis in southwestern Spain: An approach to establish the  
26 recurrence period. *Geomorphology* 203:97–104.  
27 <https://doi.org/10.1016/j.geomorph.2013.09.008>
- 28 Sabatier P, Dezileau L, Colin C, et al (2012) 7000 years of paleostorm activity in the NW  
29 Mediterranean Sea in response to Holocene climate events. *Quaternary Research* 77:1–  
30 11. <https://doi.org/10.1016/j.yqres.2011.09.002>
- 31 Sato H, Shimamoto T, Tsutsumi A, Kawamoto E (1995) Onshore tsunami deposits caused by  
32 the 1993 Southwest Hokkaido and 1983 Japan Sea earthquakes. *pure and applied*  
33 *geophysics* 144:693–717. <https://doi.org/10.1007/BF00874390>
- 34 Scardino G, Piscitelli A, Milella M, et al (2020) Tsunami fingerprints along the Mediterranean  
35 coasts. *Rendiconti Lincei Scienze Fisiche e Naturali* 1–17
- 36 Scheffers A, Kelletat D, Scheffers S (2010) Wave-emplaced coarse debris and megaclasts in  
37 Ireland and Scotland: Boulder transport in a high-energy littoral environment: A reply.  
38 *The Journal of Geology* 118:705–709

- 1 Scheffers AM (2015) Chapter 3 - Paleotsunami Research—Current Debate and Controversies.  
2 In: Shroder JF, Ellis JT, Sherman Risks and D Douglas JBT-Coastal and Marine  
3 Hazards (eds). Elsevier, Boston, pp 59–92
- 4 Scheffers AM, Kinis S (2014) Stable imbrication and delicate/unstable settings in coastal  
5 boulder deposits: Indicators for tsunami dislocation? *Quaternary International* 332:73–  
6 84. <https://doi.org/10.1016/j.quaint.2014.03.004>
- 7 Schneider H, Höfer D, Trog C, et al (2010) Holocene estuary development in the Algarve  
8 Region (Southern Portugal) - A reconstruction of sedimentological and ecological  
9 evolution. *Quaternary International* 221:141–158.  
10 <https://doi.org/10.1016/j.quaint.2009.10.004>
- 11 Schwarzer K (2020) Chapter 7 - Geophysical prospection and sedimentological characteristics  
12 of subaquatic tsunami deposits. In: Engel M, Pilarczyk J, May SM, et al. (eds)  
13 *Geological Records of Tsunamis and Other Extreme Waves*. Elsevier, pp 115–142
- 14 Sedrati M, Morales JA, El M'rini A, et al (2022) Using UAV and Structure-From-Motion  
15 Photogrammetry for the Detection of Boulder Movement by Storms on a Rocky Shore  
16 Platform in Laghdira, Northwest Morocco. *Remote Sensing* 14:4102.  
17 <https://doi.org/10.3390/rs14164102>
- 18 Sen Gupta BK (2003) *Modern Foraminifera*. Springer Netherlands, Dordrecht
- 19 Serpelloni E, Vannucci G, Pondrelli S, et al (2007) Kinematics of the Western Africa-Eurasia  
20 plate boundary from focal mechanisms and GPS data. *Geophysical Journal International*  
21 169:1180–1200. <https://doi.org/10.1111/j.1365-246X.2007.03367.x>
- 22 Shi S, Dawson AG, Smith DE (1991) Sedimentology of a Holocene tsunami deposit. Beijing,  
23 pp 329–329
- 24 Shinozaki T, Sawai Y, Hara J, et al (2016) Geochemical characteristics of deposits from the  
25 2011 Tohoku-oki tsunami at Hasunuma, Kujukuri coastal plain, Japan. *Island Arc*  
26 25:350–368. <https://doi.org/10.1111/iar.12159>
- 27 Simonet R, Tanguy R (1956) Etude statistique de la houle dans les différents ports marocains  
28 pour la période 1928–1952. *Annales du Service de Physique du Globe et de*  
29 *Météorologie, Institut Scientifique Chérifien* 16:109–130
- 30 Snoussi M, Ouchani T, Niazi S (2008) Vulnerability assessment of the impact of sea-level rise  
31 and flooding on the Moroccan coast: The case of the Mediterranean eastern zone.  
32 *Estuarine, Coastal and Shelf Science* 77:206–213.  
33 <https://doi.org/10.1016/j.ecss.2007.09.024>
- 34 Spiske M, Piepenbreier J, Benavente C, Bahlburg H (2013) Preservation potential of tsunami  
35 deposits on arid siliciclastic coasts. *Earth-Science Reviews* 126:58–73.  
36 <https://doi.org/10.1016/j.earscirev.2013.07.009>
- 37 Spiske M, Tang H, Bahlburg H (2019) Post-depositional alteration of onshore tsunami deposits  
38 – Implications for the reconstruction of past events. *Earth-Science Reviews* 103068–  
39 103068. <https://doi.org/10.1016/j.earscirev.2019.103068>



- 1 Sujatha CH, Aneeshkumar N, Renjith KR (2008) Chemical assessment of sediment along the  
2 coastal belt of Nagapattinam , Tamil Nadu , India , after the 2004 tsunami. 95:
- 3 Switzer AD, Jones BG (2008) Large-scale washover sedimentation in a freshwater lagoon from  
4 the southeast Australian coast: Sea-level change, tsunami or exceptionally large storm?  
5 *Holocene* 18:787–803. <https://doi.org/10.1177/0959683608089214>
- 6 Szczuciński W, Niedzielski P, Kozak L, et al (2007) Effects of rainy season on mobilization of  
7 contaminants from tsunami deposits left in a coastal zone of Thailand by the 26  
8 December 2004 tsunami. *Environmental Geology* 53:253–264.  
9 <https://doi.org/10.1007/s00254-007-0639-4>
- 10 Szczuciński W, Niedzielski P, Rachlewicz G, et al (2005) Contamination of tsunami sediments  
11 in a coastal zone inundated by the 26 December 2004 tsunami in Thailand.  
12 *Environmental Geology* 49:321–331. <https://doi.org/10.1007/s00254-005-0094-z>
- 13 Szczuciński W, Pawłowska J, Lejzerowicz F, et al (2016) Ancient sedimentary DNA reveals  
14 past tsunami deposits. *Marine Geology* 381:29–33.  
15 <https://doi.org/10.1016/j.margeo.2016.08.006>
- 16 ten Brink US, Chaytor JD, Geist EL, et al (2014) Assessment of tsunami hazard to the U.S.  
17 Atlantic margin. *Marine Geology* 353:31–54.  
18 <https://doi.org/10.1016/j.margeo.2014.02.011>
- 19 Terry JP, Lau AYA, Etienne S (2013) Reef-Platform Coral Boulders: Evidence for High-  
20 Energy Marine Inundation Events on Tropical Coastlines
- 21 Theilen-Willige B, Ait malek H, Ait Ougougdal M, et al (2013) Use of RapidEye-Data for the  
22 Detection of Natural Hazard Prone Areas ( Earthquake , Tsunami , Landslides ,  
23 Desertification ) in W-Morocco
- 24 Trakadas A (2015) Fish-salting in the northwest Maghreb in antiquity : a gazetteer of sites and  
25 resources. 159–159
- 26 Viles H, Spencer T (2014) Coastal problems: geomorphology, ecology and society at the coast.  
27 Routledge
- 28 Vizcaino A, Gràcia E, Escutia C, et al (2006) Characterizing Holocene paleoseismic record in  
29 the SW Portuguese Margin. pp 8469–8469
- 30 Walker M (2005) Quaternary dating methods. John Wiley and Sons
- 31 Yawsangratt S, Szczuciński W, Chaimanee N, et al (2012) Evidence of probable paleotsunami  
32 deposits on Kho Khao Island, Phang Nga Province, Thailand. *Natural Hazards* 63:151–  
33 163. <https://doi.org/10.1007/s11069-011-9729-4>
- 34 Yu N-T, Yen J-Y, Chen W-S, et al (2016) Geological records of western Pacific tsunamis in  
35 northern Taiwan: AD 1867 and earlier event deposits. *Marine Geology* 372:1–16.  
36 <https://doi.org/10.1016/j.margeo.2015.11.010>
- 37 Zitellini N, Chierici F, Sartori R, Torelli L (1999) The tectonic source of the 1755 Lisbon  
38 earthquake and tsunami. *Annals of Geophysics* 42:. <https://doi.org/10.4401/ag-3699>

